Volume 3 | Number 5 | September 2016 | Pages 365–462

Materials Horizons

rsc.li/materials-horizons

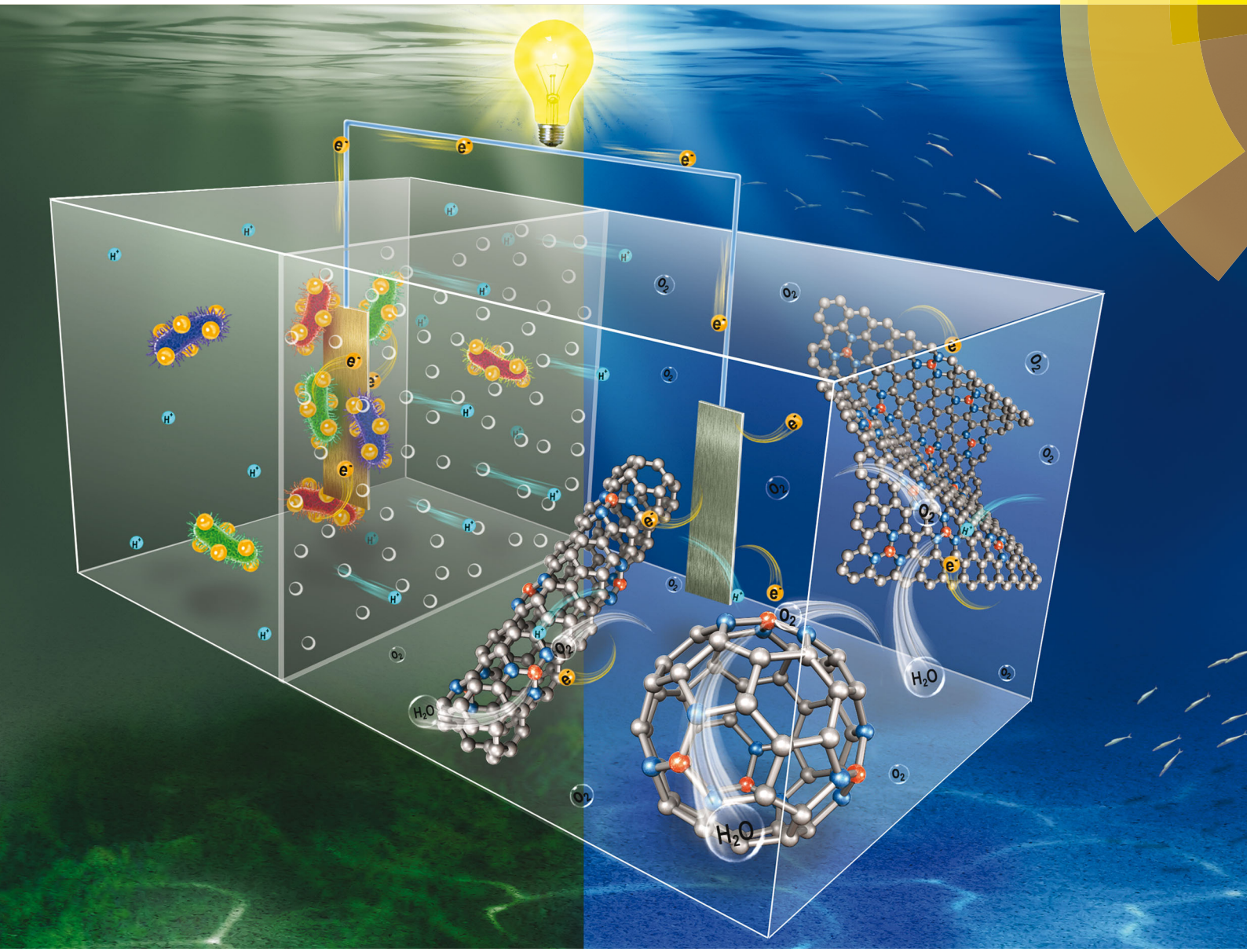

ISSN 2051-6347

ROYAL SOCIETY OF CHEMISTRY

REVIEW ARTICLE
Yang Hou, Junhong Chen, Zhen He *et al.*
Oxygen reduction reaction catalysts used in microbial fuel cells for energy-efficient wastewater treatment: a review

175 YEARS

Materials Horizons

REVIEW

View Article Online
View Journal | View Issue

Cite this: *Mater. Horiz.*, 2016, 3, 382

Oxygen reduction reaction catalysts used in microbial fuel cells for energy-efficient wastewater treatment: a review

Heyang Yuan,[a] Yang Hou,*[b] Ibrahim M. Abu-Reesh,[c] Junhong Chen*[d] and Zhen He*[a]

Received 31st March 2016,
Accepted 29th April 2016

DOI: 10.1039/c6mh00093b

www.rsc.li/materials-horizons

Microbial fuel cells (MFCs) as an energy-efficient wastewater treatment technology have attracted increasing interest in the past decade. Cathode catalysts for the oxygen reduction reaction (ORR) present a major challenge for the practical applications of MFCs. An ideal cathode catalyst should be scalable, durable, and cost-effective. A variety of non-precious metal catalysts have been developed for MFC applications, including carbon-based catalysts, metal-based catalysts, metal–carbon hybrids, metal–nitrogen–carbon complexes, and biocatalysts. This paper comprehensively reviews these materials with emphasis on their synthesis, performance, durability, and cost. It is anticipated that insights offered in this review could facilitate the development of ORR catalysts for MFC applications towards energy-efficient wastewater treatment.

[a] *Department of Civil and Environmental Engineering, Virginia Polytechnic Institute and State University, Blacksburg, VA 24061, USA. E-mail: zhenhe@vt.edu*
[b] *Department of Chemistry and Food Chemistry & Center for Advancing Electronics Dresden (CFAED), Technische Universitaet Dresden, 01062 Dresden, Germany. E-mail: houyang1213@hotmail.com*
[c] *Department of Chemical Engineering, College of Engineering, Qatar University, P.O. Box 2713, Doha, Qatar*
[d] *Department of Mechanical Engineering, University of Wisconsin-Milwaukee, 3200 North Cramer Street, Milwaukee, Wisconsin 53211, USA. E-mail: jhchen@uwm.edu*

1. Introduction

The growing demand for water and energy has become a critical issue for sustainable societal development in the 21st Century. Globally there are 783 million people lacking access to clean water and 2.5 billion people lacking adequate water sanitation.[1] Meanwhile, electricity is unavailable to more than 1.3 billion people.[1] There is a strong nexus between water and energy. For example, water and wastewater utilities consume 3% of the

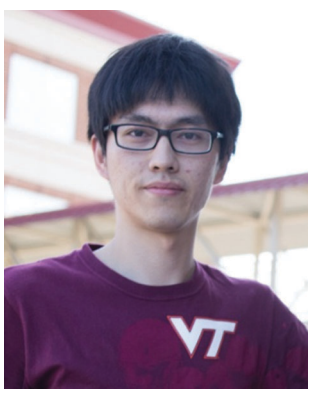

Heyang Yuan

Mr Heyang Yuan is now a PhD student advised by Dr Zhen He in the Via Department of Civil and Environmental Engineering at Virginia Polytechnic Institute and State University (Virginia Tech). He received his BS from Tongji University and MS from Technische Universitaet München, where he has conducted research in microbial communities in activated sludge. At Virginia Tech, his research focuses on fundamentals and optimization of microbial desalination cells and nano-structured materials for electrode/catalyst application in bioelectrochemical systems.

Yang Hou

Dr Yang Hou received his PhD degree from the School of Environmental Science & Technology of Dalian University of Technology in 2011, and then did 3.5 years of postdoctoral research in the Department of Chemistry at the University of California, Riverside, and Department of Mechanical Engineering, University of Wisconsin–Milwaukee. Now he is a research associate working with Professor Xinliang Feng in the Center for Advancing Electronics Dresden, Technische Universitaet Dresden. His current research focuses on the design and synthesis of low-dimensional nanomaterials for energy and environmental applications. He has published nearly 60 papers and is an editorial board member at Scientific Reports.

electricity in the USA, which accounts for 35% of the total municipal energy budgets.[2] On the other hand, wastewater is increasingly considered as an energy resource, and the potential energy that can be extracted from domestic wastewater is estimated to be 3.8 kW h g^{-1} COD (chemical oxygen demand).[3] This energy can be recovered as methane by anaerobic digestion, which is mainly applied to treat concentrated wastes such as sludge; however, inefficient collection of methane gas could result in the release of methane into the atmosphere as a greenhouse gas.[4] Therefore, there is an urgent need to develop energy-efficient and environmentally-friendly methods for sustainable wastewater treatment.

Microbial fuel cells (MFCs) are green technologies that can directly convert the organic energy in wastewater into electricity.[5] Similar to chemical fuel cells, MFCs are composed of an anode and a cathode (Fig. 1). The electrochemically active microorganisms (*i.e.*, exoelectrogens) that grow in the anode are fed by the organic matter in wastewater and respire extracellularly by transferring electrons to the anode electrode.[6] When an appropriate electron acceptor (*e.g.*, oxygen) is present in the cathode and the overall thermodynamics of the cell is favourable, the electrons flow spontaneously through the external circuit to the cathode for reduction reactions. As such, electrical energy is produced and wastewater is treated. Compared to conventional activated sludge processes, MFCs can theoretically achieve a positive energy balance and produce significantly less waste sludge, which further enhances energy efficiency.[7] Moreover, the electricity produced by MFCs is cleaner than CH_4 in terms of greenhouse effects.

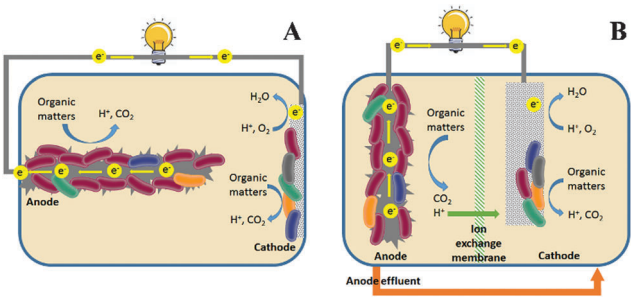

Fig. 1 Schematic of (A) single-chamber MFCs and (B) two-chamber MFCs.

One of the main challenges is the development of efficient and stable cathode catalysts for MFCs.[8] Oxygen is an ideal electron acceptor for MFCs because of its high redox potential, availability, and sustainability. However, the oxygen reduction reaction (ORR) is kinetically sluggish, resulting in a large proportion of potential loss.[9] Although platinum (Pt) shows a high ORR catalytic activity, a Pt-based cathode could account for more than 50% of the total capital cost of lab-scale MFCs, and thus it is not economically viable for large-scale wastewater treatment.[10] A number of materials have been studied as alternative ORR catalysts for MFCs. Recent publications have reviewed these

Ibrahim M. Abu-Reesh

Professor Ibrahim M. Abu-Reesh received his master's and doctorate degrees from the Chemical Engineering Department at Washington University, St. Louis, Missouri, USA, and his BSc degree in petroleum refining engineering from Suez Canal University, Egypt. Dr Abu-Reesh has taught in chemical engineering departments for about 20 years before joining Qatar University (Fall 2011) at institutions such as the University of Jordan, King Fahd University of Petroleum and Minerals, and the American University of Sharjah, as a visiting professor. Dr Abu-Reesh's research publications are in the area of biochemical engineering and environmental biotechnology.

Junhong Chen

Junhong Chen is a Distinguished Professor of Mechanical Engineering and Materials Science and Engineering at the University of Wisconsin–Milwaukee, and a Fellow of American Society for Mechanical Engineers (ASME). He is also the Director of the Industry-University Cooperative Research Center (I/UCRC) on Water Equipment and Policy, supported by the U.S. National Science Foundation (NSF) and water-based industrial partners. His research interests lie in nanostructure-based sensors and nanocarbon-based hybrid nanomaterials for sustainable energy and environment (http://www.uwm.edu/nsee/).

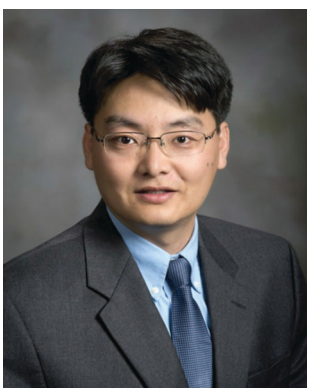

Zhen He

Dr Zhen He is an Associate Professor in the Via Department of Civil and Environmental Engineering at Virginia Tech. Prior to this position, he was an Assistant Professor of Civil Engineering and Mechanics at the University of Wisconsin–Milwaukee. He received his BS from Tongji University, MS from the Technical University of Denmark, and PhD from Washington University in St. Louis, and all of them were in environmental engineering. His research focuses on the development of biotechnologies for sustainable water and wastewater treatment. He has published more than 100 journal papers and is an associate editor for Water Environment Research.

catalysts from the perspectives of their structures and the ORR mechanisms,[11–14] but the unique features of the ORR catalysts for MFC applications are not well demonstrated. Furthermore, the role of MFCs as a research platform in evaluating the activity and durability of catalysts remains to be explained.

This review comprehensively summarizes the ORR catalysts used in MFCs with a focus on their synthesis/modification procedure, durability, performance, stability, and economics. The criteria that ORR catalysts should meet for MFC applications and the evaluation methods based on MFC experiments are demonstrated. The cathode catalysts are categorized into carbon-based catalysts, metal-based catalysts, carbon–metal hybrids, metal–nitrogen–carbon complexes and biocatalysts. The synthesis/modification, the consequently enhanced performance, and the stability of the catalysts are discussed in detail. The costeffectiveness of the catalysts is interpreted as the maximum power density (MPD) normalized to the cost for comparison. This review is expected to provide insights into the development of ORR catalysts for MFC-based wastewater treatment.

2. ORR catalysts used in MFCs

The ideal ORR catalysts used in MFCs are expected to be cost-effective and have high catalytic activity, because MFCs are engineered primarily for wastewater treatment, and thus the capital and maintenance costs should be comparable to conventional treatment technologies.[7] At this stage of development, the energy generated by MFCs is mainly used to balance the energy consumption rather than to generate additional economic benefits,[15] further highlighting the importance of economic feasibility of the cathode catalysts. Hence, properties associated with practicality, including simple and large-scale synthesis, low cost, and high durability should be given priority when developing ORR catalysts for MFC applications.

Besides their cost effectiveness, the durability of the ORR catalysts in MFCs is another major challenge, because the cathode is constantly exposed to wastewater containing organic matter, contaminants and microorganisms. In single-chamber MFCs (Fig. 1A), the catalysts directly contact the wastewater and may be poisoned by the intermediate products such as methanol, chloride, sulfide, *etc.*[16–18] Furthermore, organisms can form a biofilm on the cathode surface and degenerate catalytic performance by blocking the O_2 transport.[19,20] Although in some circumstances the biofilm may serve as a biocatalyst,[21] the interaction between the organisms and the catalyst remains unknown and warrants further studies. Similar problems are also found in two-chamber MFCs (Fig. 1B), where the anode effluent is commonly introduced into the cathode for post-treatment.[22] Poisoning of the catalysts by intermediates leads to high potential loss and reduced power production. Previous studies showed an increased CH_4 production at a lower current, indicating the competition for substrates between exoelectrogens and methanogens.[23] To make MFCs for practical applications, the ORR catalysts must be tolerant to poisoning, resistant to biofouling and able to restore catalytic activity after cleaning.

Whilst ORR catalysts are developed to enhance MFC performance, MFCs also present a powerful tool to study the durability and activity of the catalysts. The assessment using MFCs provides insightful information that cannot be obtained by *ex situ* electrochemical characterization methods. For example, multi-cycle cyclic voltammetry (CV) as a method to measure durability is typically accomplished with 6000–10 000 cycles in ~48 h depending on the scan rate, which is much shorter than the operation period of MFCs (*i.e.*, several weeks to months). Similarly, the chronoamperometric curve for assessing catalytic stability lasts only a few hours, and the typical operation potential (*e.g.*, −0.4 V *vs.* Ag/AgCl) is much more negative than that in MFCs (*i.e.*, ~0 V *vs.* Ag/AgCl). Electrochemical impedance spectrometry (EIS) can be used to measure the distribution of internal resistance,[24] but the overall internal resistance for calculating the MPD cannot be obtained. In contrast, the measurement of the polarization curve and cathode potential in MFCs not only yields the overall internal resistance, but can also be used for comparison of the concentration overpotential at high current output.[25] Moreover, long-term MFC experiments help gain a better understanding of the complicated effects of poisoning and fouling caused by real wastewater.[26–28]

It should be noted that the choice of external resistance is critical when performing MFC experiments. The difference in current production between the catalysts of interest and the control Pt/C is artificially diminished by using a large resistance (Fig. 2). As aforementioned, the current will determine the anode potential and will consequently affect the microbial activity, metabolite production and fouling. It is thus recommended that, when evaluating the long-term stability, MFCs should be operated at a high current mode (*i.e.*, low external resistance) and/or a high power mode (*i.e.*, external resistance equals the internal resistance), which are the typical operational conditions in real applications.

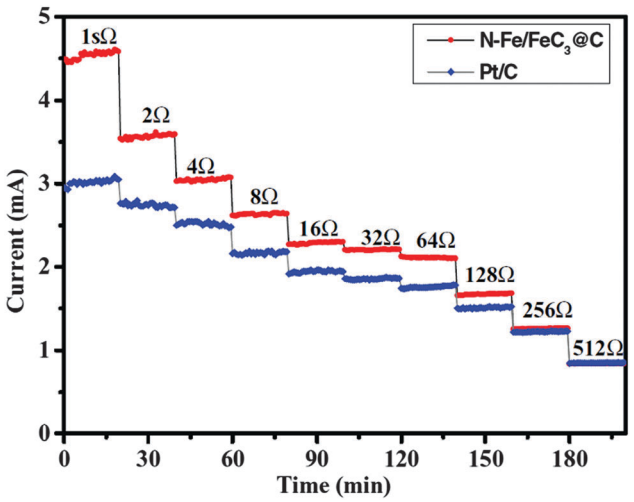

Fig. 2 Current production as a function of external resistance. Reproduction with permission from ref. 29. Copyright (2012) John Wiley & Sons.

3. Carbon-based catalysts

3.1 Carbon black

Carbon black (CB) is a product from incomplete combustion or thermal decomposition of hydrocarbons.[30] Due to its high stability and large specific surface area, CB is widely used as the support material for metal catalysts.[31] However, simple chemical modification and/or the introduction of functional groups can create active sites that make CB itself a metal-free ORR catalyst.

In a study treating CB with nitric acid, the MPD of the MFC equipped with the modified CB was 3.3 times that with pristine CB and was 78% of that with Pt/C.[32] A similar enhancement in MPD (71% of that with Pt/C) was reported in another study by using nitric acid and ammonia gas as treatment reagents, which was likely attributed to the successful introduction of oxygen and nitrogen atoms on the CB surface.[33] Pyrolyzing CB and polytetrafluoroethylene (PTFE) under an ammonium atmosphere resulted in the co-doping of nitrogen and fluorine atoms.[34] As a consequence, the electron transfer number increased from 2.7 for the un-doped CB to 3.8 for the co-doped one, and the MPD of the MFC with the treated CB reached 672 mW m^{-2}, which was 1.2 times that with Pt/C.

CB as a cathode catalyst shows high economic viability. For example, polypyrrole/carbon black (PPy/C) yielded a MPD that is 70% of that with Pt/C. When the MPD was normalized to the material cost, the composite was 15 times more efficient than Pt/C.[35] Despite the excellent cost effectiveness, the durability of CB catalysts in MFCs remains unknown. Furthermore, systematic doping of heteroatoms (N, O, S, P, *etc.*) in CB for improving catalytic activity warrants further studies.

3.2 Activated carbon

Activated carbon (AC) refers to porous carbon materials (surface area $>$ 1000 m^2 g^{-1}) that are produced by the thermal or chemical activation of a wide range of carbonaceous precursors.[36] The preparation of AC from silk fibroin was the first study showing that AC could catalyse ORR, which was attributed by the authors to the intrinsic nitrogen atoms.[37] Later, peat-based AC was used as the MFC catalyst and achieved a MPD of 1220 mW m^{-2}, 1.2 times that with Pt/C, indicating that AC might hold great promise for MFC applications.[38] The results of the two studies also suggest that AC produced from different precursors will possess different chemical functional groups, BET specific surface areas and active sites, which may synergistically affect ORR catalysis. AC made from five precursors, including peat, coconut shell, hardwood carbon, phenolic resin and bituminous coal, were examined as the ORR catalysts in MFCs and yielded varied performance.[39] The AC derived from bituminous coal performed relatively poorly in terms of onset potential (0.09 V *vs.* Ag/AgCl) and electron transfer number (2.4), but generated the highest MPD (77% of Pt/C) among those AC. It was found that the content of strong acid functional groups in the AC negatively correlated with the onset potential, while the BET specific surface area could not be used to predict the catalytic performance. A similar conclusion on the surface area was drawn by another study on AC produced from six different precursors.[40] Interestingly, both studies observed high oxygen contents (4–10%), but negligible-to-no nitrogen in the AC, leaving the ORR catalysis mechanisms to be further understood.

A number of modifications of AC have been carried out to overcome the limitations caused by the precursors. For instance, simple physical modification by blending CB with AC presents an effective method to reduce both the ohmic and charge transfer resistances, thereby increasing the MPD by 16% compared to bare AC.[41] Chemical treatment with alkali or acid has also been reported to enhance ORR performance *via* the formation of possible chemical bonds. The AC pre-treated with potassium hydroxide reduced the internal resistance and yielded a MPD 16% higher than the untreated AC, possibly because of the increased electrolyte–catalyst affinity caused by the adsorbed OH^-.[42] Meanwhile, the pre-treatment of AC with phosphoric acid at 80 and 400 °C showed 35% and 55% increase in the MPD, respectively.[43] The introduction of non-acidic oxygen content and P in the form of C–O–P bonding might account for the improved catalysis.[44,45] On the other hand, the acidic functional groups resulting from H_3PO_4 treatment were speculated to be detrimental to ORR catalysis,[44] consistent with the findings in those studies using AC from different precursors.[39]

Treatment using nitrogen-containing chemicals is one of the most effective methods for improving the ORR catalysis of AC as it can achieve multiple benefits. Treating AC in ammonia gas at 700 °C not only removed oxygen functional groups, but also introduced nitrogen atoms, leading to a MPD (2450 mW m^{-2}) 28% higher than untreated AC and 16% higher than Pt/C, respectively.[46] Nitrogen doping has been demonstrated to be an effective strategy to enhance catalytic activity.[47] Three different types of doped nitrogen may play important roles in ORR catalysis: graphitic-N may favor the reduction of O_2 to H_2O_2 *via* the $2e^-$ pathway, whereas pyridinic- and pyrrolic-N are likely to contribute to the $4e^-$ pathway.[48,49] A recent study reported an N-doped AC catalyst with a remarkably high nitrogen content (8.65% total N and 5.56% pyridinic-N) by acid/alkaline pre-treatment and using cyanamide as the nitrogen precursor (Fig. 3).[50] The modified AC achieved an electron transfer number of 3.99 and a MPD (650 mW m^{-2}) 44% higher than Pt/C. In addition to nitrogen-doping, nitrogen-containing chemicals such as ammonium bicarbonate could serve as a pore former to increase porosity and alter pore size distribution, which could reduce charge transfer resistance and consequently enhance the MFC performance.[51]

AC as an ORR catalyst exhibits excellent electrochemical durability. While the current density of a Pt/C cathode dropped by 73% after 7 h of the chronoamperometry test, a nitrogen-doped AC cathode showed only 30% decrease.[50] However, biofouling on the AC cathode and degenerated MFC performance were still observed.[40] The disinfectant quaternary ammonium compound was added in AC to inhibit biofilm growth.[52] After 2 months of operation, the protein content on the modified AC cathode was 26 times lower than that on the control electrode, leading to a lower charge transfer resistance (Fig. 4) and a more stable MPD. Long-term studies suggested that the MPD of the MFCs using

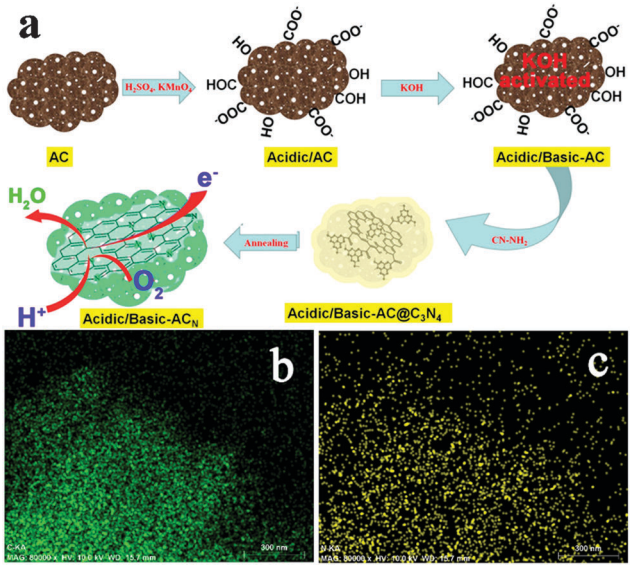

Fig. 3 (a) The synthesis of the acidic/basic-AC_N, (b) the carbon element mapping, and (c) the nitrogen element mapping. Reproduction with permission from ref. 50. Copyright (2014) American Chemical Society.

an AC–CB mixture as the cathode catalysts decreased by only 1–7% after 5 months of operation.[41,53] After 16 months of operation, the performance of AC–CB dropped to 79% of its original level, but could be recovered to 90% using a simple acid washing (60 mM HCl solution).[53] On the other hand, acid cleaning did not noticeably recover the performance of Pt/C cathodes, which generated a MPD only 21% of its initial value.

AC has attracted much attention due to its high cost effectiveness. Compared to commercial Pt/C, whose price is \$28 g^{-1} (10% Pt on Vulcan XC 72, Premetek Co., Wilmington, DE, USA) and the normalized MPD is only ~1 mW $\$^{-1}$ (with a typical loading rate of 5 mg cm^{-2}), AC costs less than \$0.002 g^{-1}. The unit price of the AC blended with CB was lower than \$1 m^{-2}, together with the high power production leading to a normalized MPD of 1210 mW $\$^{-1}$.[53] It was also estimated that a complete

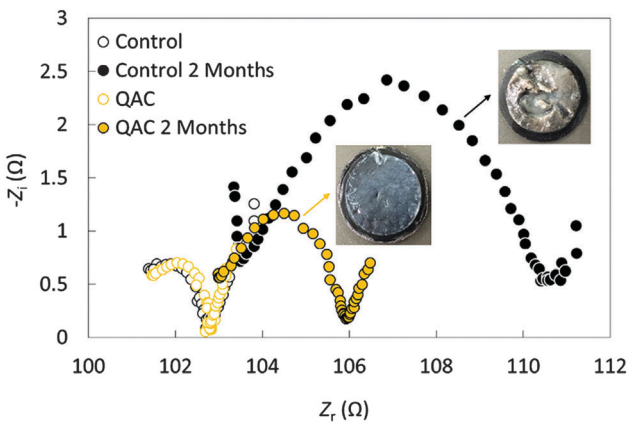

Fig. 4 Nyquist plots of the control and QAC before and after 2 months of operation. Reproduction with permission from ref. 52. Copyright (2014) Elsevier.

AC cathode, including the AC catalyst, the PTFE binder and the metal support, costs \$30–60 m^{-2}, which resulted in a normalized MPD of 22–41 mW $\$^{-1}$ depending on the MFC performance.[54,55] The normalized MPD could be further improved to 94–98 mW $\$^{-1}$ by pressing AC–PTFE on a stainless steel mesh,[56] or by phase inversion of an AC/CB/PVDF (poly(vinylidene fluoride)) mixture,[57] demonstrating its potential for practical applications.

3.3 Carbon nanofibers/nanotubes

Carbon nanofibers (CNFs) are composed of stacked corn-shaped graphene sheets and show high electrical conductivity and a high BET specific surface area.[58,59] Similar to the treatment of AC, alkaline/acid activation and nitrogen doping are common strategies to improve the ORR catalysis of CNFs. Immersing CNFs into 8 M KOH solution increased its surface area from 275 m^2 g^{-1} to 2100 m^2 g^{-1}, and consequently enhanced the MPD by 79% with respect to the untreated CNFs.[60] By comparison, HNO_3 treatment of CNFs did not significantly change the BET surface area, but shifted the pore size distribution, which might favor ORR catalysis.[61] Nitrogen-doped CNFs *via* the pyrolysis of pyridine showed high catalytic activity and obtained a MPD comparable to that with Pt/C.[62] The combination of nitrogen doping and chemical activation with KOH yielded a CNF material with a large BET surface area (1984 m^2 g^{-1}) and high catalytic activity (electron transfer number 3.6), and the MFC equipped with the modified CNFs generated a MPD (1377 mW m^{-2}) similar to that of the Pt/C-based MFC.[63] Recently, heteroatom-doped porous CNFs were obtained *via* the pyrolysis of natural spider silk (Fig. 5).[64] Owing to the abundant electronegative N and S atoms within the carbon lattice and the high BET surface area (721.6 m^2 g^{-1}), the CNFs achieved a MPD of 1800 mW m^{-2}, 1.6 times higher than Pt/C.

Carbon nanotubes (CNTs) are one or multiple layers of graphene sheets wrapped in a concentric manner,[65,66] whose catalytic activity can be tuned by heteroatom doping.[67] It has been reported that vertically aligned nitrogen-doped CNTs catalyse ORR mainly *via* the $4e^-$ pathway.[68] The N-doped CNTs showed lower internal resistance and a more positive onset potential in cyclic voltammetry tests compared to Pt/C.[69] The MFCs with the N-doped CNTs thus outperformed the Pt/C-MFCs in terms of power production. Quantum mechanics calculations suggested that nitrogen dopants increased the positive charge density of carbon atoms and induced charge delocalization, which could enhance parallel diatomic adsorption of O_2 and weaken O–O bonds during ORR catalysis.[70] In addition to pre-treatment and nitrogen doping, mixing CNTs with a conductive polymer, such as polyaniline (PANI) or polypyrrole (PPy), presents a simple method to enhance the cathode performance.[71,72] Although the ORR catalysis of those CNT/polymer composites was slightly inferior to that of N-doped CNTs and Pt/C, the simple and large-scale production makes them competitive catalysts for practical applications.

Both CNFs and CNTs as cathode catalysts are more durable than Pt/C. Activated N-doped CNFs showed less attenuation than Pt/C in chronoamperometry tests, likely because the graphitic-N in the carbon plane was less susceptible to protonation.[63]

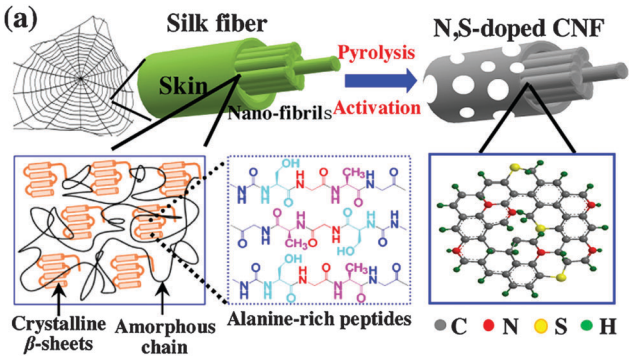

Fig. 5 The synthesis of heteroatom-doped CNFs derived from spider silk. Reproduction with permission from ref. 64. Copyright (2016) Elsevier.

With respect to long-term stability, the Pt/C cathode severely deteriorated due to sulfide poisoning and biofilm growth, but the activated CNF cathode showed only a slight decrease in the MPD.[61] The CNF synthesized using spider silk was not affected by the crossover effects of various chemicals (*e.g.* formate, ethanol, lactate, methanol, acetate, sulfide, and ascorbate), and constantly produced high MPD in 3 months of continuous operation.[64]

The cost of CNFs prepared by the electrospinning of polyacrylonitrile was estimated to be \$7.5 g^{-1}, and increased slightly to \$9.6 g^{-1} after KOH treatment; but the normalized MPD of the modified CNFs was still 2.6 times that with Pt/C.[60] The normalized MPD of the polyaniline/multi-walled CNT composite reached 31 mW $\$^{-1}$ owing to the low cost of commercial multi-walled CNTs.[71] However, CNFs and CNTs were still not competitive to AC. The CNFs obtained from spider silk used free natural materials and might provide insight into the cost-effective fabrication of sustainable cathode catalysts.

3.4 Graphite/graphene

Graphite is multiple layers of carbon sheets bonded through weak van der Waals interaction. Due to its high electrical conductivity and high stability, graphite is commonly used as a fuel cell electrode.[73] Exfoliation of graphite can form single-layer carbon nanosheets known as graphene.[74] The discovery of graphene was awarded the 2010 Nobel Prize for Physics and has drawn extensive attention in the past decade.[75,76] With high electrical conductivity and a high BET surface area, graphene-based cathode catalysts have been demonstrated to effectively catalyse the ORR in MFCs.[14]

Pristine graphite is not considered catalytic toward the ORR because of the lack of active sites. However, the MFC filled with granular graphite generated a stable MPD of 50 W m^{-3}, comparable to many common catalysts.[77] Furthermore, the COD removal (1.46 kg m^{-3} d^{-1}) by the graphite-based MFC was higher than that of conventional aerobic processes, which was of practical significance for wastewater treatment. Activation of graphite with HNO_3 and H_3PO_4 could enhance the MPD by 2 and 2.4 times, respectively.[78,79] In another study, the graphite treated with HNO_3 achieved a MPD similar to that with Pt/C, which could be attributed to the high BET surface area of the modified graphite and the introduction of nitrogen and oxygen functional groups.[80]

The modification of graphene has mainly focused on the doping of heteroatoms. Detonation of cyanuric chloride and trinitrophenol could effectively incorporate three different nitrogen species (*i.e.*, pyridinic-N, pyrrolic-N, and graphitic-N) in graphene, leading to a high electron transfer number of 3.7.[81] Implantation of mesoporous graphitic carbon nitride in N-doped graphene further enhanced the catalytic activity (complete $4e^-$ ORR pathway), and yielded a MPD of 1618 mW m^{-2}, 14% higher than Pt/C.[82] The co-doping of nitrogen and sulfur in carbon could provide dual active sites for ORR catalysis.[83] The N/S co-doped carbon nanosheets produced a lower MPD but a comparable current density to Pt/C, suggesting that this catalyst could be used in bioelectrochemical systems that require high current output.[84] Graphene and N-doped graphene generally have a relatively low surface area, which can be increased by using KOH activation.[85] A more direct way to increase the BET surface area is to prepare crumpled graphene particles by capillary compression in rapidly evaporating aerosol droplets.[86,87]

Similar to other carbon catalysts, both graphite and graphene catalysts exhibit high stability. In the presence of sulfide, the MPD using N-doped graphite as the cathode catalyst was not affected and became similar to that using Pt (Fig. 6a).[26] Compared to the 17% decrease in the MPD of Pt/C-MFC after 35 cycles, the MPD of the MFC with N-doped graphene decreased by only 9%.[81] It was further reduced to 4% by implanting C_3N_4 in the N-doped graphene.[82] It was proposed that the oxygen species introduced during the synthesis of N-doped graphene could protect catalytic C–N groups from being attacked by protons, which might account for the superior stability (Fig. 6b).[88]

The cost effectiveness of graphite and graphene is comparable to that of CNFs/CNTs, but still less competitive to AC. Based on the literatures, the normalized MPD is approximately 12 mW $\$^{-1}$ for granular graphite,[77] and 10 mW $\$^{-1}$ for N/S co-doped carbon nanosheets.[84] The major problem of the heteroatom-doped graphene lies in its complicated synthesis process and low yields. In the typical procedures, graphene oxide is first prepared, reduced to graphene and then subjected to modification.[89] Other synthesis methods such as chemical vapor deposition, unzipping of MWCNTs and detonation, *etc.* are either energy/time-consuming or involve hazardous chemicals.[90,91]

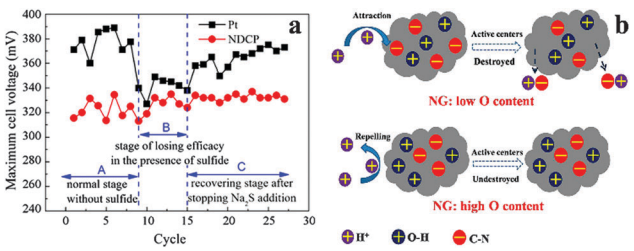

Fig. 6 (a) The maximum cell voltage evolution in a typical three-stage process. Reproduction with permission from ref. 25 and 26. Copyright (2012) Elsevier. (b) Proposed mechanism for the improvement of long-time activity of N-doped graphene by O–H groups. Reproduction with permission from ref. 88. Copyright (2013) American Chemical Society.

Therefore, a facile and efficient approach to creating graphene-based catalysts is highly desired and should be the focus of future studies.

3.5 Carbon synthesized from sustainable precursors

In addition to the well-defined categories, many other carbon materials have been developed using a variety of sustainable precursors, including biochar obtained from the pyrolysis of sewage sludge;[92,93] the heteroatom-doped carbon derived from cellulose,[94–96] dopamine,[97] straw,[98] chitin,[99] and petroleum coke;[100] and the carbon nanoparticle-coated porous biocarbon prepared from plant moss.[101] The MFCs equipped with these carbon catalysts have shown a high electron transfer number and comparable or superior catalytic performance to Pt/C. For example, three cellulose-based catalysts generated MPDs ranging from 1041 to 2293 mW m^{-2} due to the different MFC configurations, but all outperformed their control MFCs using Pt/C.[94–96]

This group of carbon cathodes is of particular interest, because they meet the requirement of durability and economy besides their high activity. Chitin-based carbon sheets were tolerant to methanol crossover, and the voltage output remained 97% of its original value after 60 days of operation.[99] The moss-based biocarbon was also tolerant to methanol and showed considerable stability in chronoamperometric tests.[101] The normalized MPD of the moss-based biocarbon may even be competitive to AC, as its precursor is free and readily available. According to the estimated price, loading rate and power production, the normalized MPD of N/P co-doped cellulose carbon could reach up to 143 mW $\$^{-1}$,[95] highlighting its feasibility for MFC practical applications.

4. Metal-based catalysts

4.1 Metals and alloys

Many pure metals exhibit strong ORR catalytic activity. For example, noble metal Pt is considered to be the most active catalyst using the theoretical calculation of O_2-, O-, and OH-binding energy,[102] and it is proposed to catalyse the ORR *via* a dissociative mechanism at a low current density and an associative mechanism at a high current density, both of which are $4e^-$ pathways.[103] Many efforts have been devoted to reduce the amount of Pt loading on the MFC cathode without compromising the catalytic performance. The deposition of Pt on carbon paper by electron beam evaporation reduced the thickness of the Pt layer and minimized Pt loading, but significantly increased the current output of the MFC.[104] A more practical way of reducing the loading is to alloy Pt with inexpensive transition metals, such as Fe,[105] Co and Ni,[106] which has been studied to further reduce the oxygen binding energies and enhance the catalytic activity.[107] With appropriate Pt : metal ratios, Pt-based alloys could generate higher MPDs than commercial Pt/C.[108,109]

The stability of the metal catalysts presents the most challenging issue that hinders their commercial applications. Leaching of metallic Co from Pt–Co alloy was observed under an acidic electrochemical environment.[108] Similar degeneration occurred for a Pt–Fe alloy, although its MPD in MFCs under neutral conditions was more stable than that with Pt/C.[109] To cope with the possible biofouling, silver nanoparticles were used as the cathode catalysts and antimicrobial agents.[110] It was observed that the biomass attached on the AgNP-coated cathode after 50 days was 44% less than that on plain graphite and 25% less than that on Pt/C (Fig. 7). The cost of metal-based catalysts is also a major concern. The use of scrap metals recycled from electronics and automobiles was sustainable and could produce a satisfactory MPD (422 mW m^{-2}), but the normalized MPD was only 0.05 mW $\$^{-1}$ due to the large quantity of materials used in the cathode.[111]

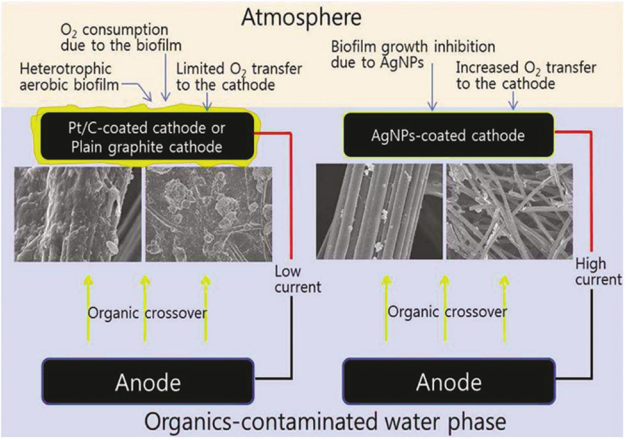

Fig. 7 Biofouling on the cathode with Pt/C, plain graphite and Ag nanoparticles. Reproduction with permission from ref. 110. Copyright (2011) American Chemical Society.

4.2 Metal oxides

Manganese dioxide has been successfully used as the cathode catalyst in aqueous and non-aqueous fuel cells for many decades.[112] It is thus not surprising to find extensive studies on MnO_2 in MFCs. However, most of the MnO_2 achieved MPDs only half of that with Pt/C, regardless of structure modifications or doping of other transition metals.[113–115] A change of the oxidation state of manganese oxides may affect the catalytic activity. Different components in MnO_x with varied manganese valences, including MnO_2, Mn_2O_3, Mn_3O_4, Mn_5O_8 and MnOOH, may coexist and contribute differently to ORR catalysis.[116] Electrochemical deposition methods could synthesize MnO_x with a lower oxidation state, thereby increasing the electron transfer number up to 3.5.[117] Meanwhile, core–shell–shell MnO_2 nanowires could facilitate electron transfer due to the interactions between the conductive middle layer and MnO_2.[118] A simple synthesis strategy using a hydrothermal method and *in situ* chemical polymerization was developed to prepare MnO_2/PPy/MnO_2 multi-walled nanotubes.[119] The modified MnO_2 catalysts showed much lower ohmic and charge transfer resistance than the pristine MnO_2 nanotube and produced a MPD close to that of Pt/C.

Spinel manganese–cobaltite, a mixed valence transition metal oxide that can be obtained using facile synthesis methods, is a

promising catalyst for the ORR under alkaline conditions.[120] This is particularly attractive for MFC applications, because it can reduce the investment on buffer solution, and consequently improve the cost effectiveness. The manganese cobaltite/PPy nanocomposite showed an electron transfer number of 3.9 in KOH electrolyte and produced a MPD 91% of that with Pt/C under neutral conditions.[121] Doping copper in spinel manganese–cobaltite could affect both the BET surface area and the ORR electron-transfer pathway, and thus could achieve an improved MFC performance.[122] Another type of spinel, manganese–ferrite, showed the complete $4e^-$ pathway after the incorporation of PANI.[123]

Many other metal oxides, such as lead dioxide,[124] perovskite oxides,[125] vanadium oxides,[126,127] cobalt oxide and zirconium oxide,[128,129] have been studied as the cathode catalysts in MFCs. Perovskite oxides produced the highest normalized MPD of 116 mW $\$^{-1}$ among those metal oxides due to their low cost ($\$0.041\ g^{-1}$).[125] However, the MPD of perovskite oxides decreased by 15% after 15 cycles, indicating that the stability of the material needed to be improved. The stability and cost of other metal oxides remain to be investigated, and the possible leaching of the metals to the treated wastewater, the toxic effects and environmental impacts should be taken into consideration.

5. Metal–carbon hybrids

5.1 Metal–AC

AC with superior electrochemical properties has increasingly been used to replace CB as the support material for metal catalysts. Mechanical mixing of MnO_2 and AC led to a reduced internal resistance, and the weight ratio was optimized to be 1 : 1.[130] The addition of ceria, an oxygen storage material, with a fractional change between Ce^{3+} and Ce^{4+}, could further improve the cathode performance.[131] Similarly, mixing Co_3O_4 or $NiCo_2O_4$ with AC resulted in an increased MPD by maintaining the high BET surface area and reducing the charge transfer resistance.[132,133] To achieve more homogeneous mixing, the non-stoichiometric Fe_3O_4 and AC were sonicated and an MPD 83% higher than the pristine AC was produced.[134]

Electrochemical deposition of MnO_2 on AC can form closer interactions between the materials, as evidenced by the varied surface area and pore size distribution of MnO_2–AC hybrids, which can be a key factor for cathode performance.[135] The same method was adopted to deposit silver on AC, and a MPD 1.7 times higher than that with bare AC was achieved.[136] The mixed components of zero-valent, monovalent and divalent Ag were hypothesized to transform mutually, thereby contributing to ORR catalysis. In another study of depositing Cu_xO, the lattice defects and stacking faults of the Cu crystal were shown to affect the electrochemical characteristics.[137] It was also found that electrodepositing Cu_2O on AC can change the surface roughness and the pore structure, and create lattice (111) planes and surface oxygen defects in n-type Cu_2O, all of which might account for the improved electro-transfer kinetics.[138] Similar to the electrodeposition strategy, chemical synthesis can incorporate metals in carbon structures and yield synergetic effects. Pyrolyzing the AC with Fe–ethylenediaminetetra acetic acid systematically decreased the surface area with increased Fe–EDTA content, but introduced N and Fe atoms into the surface structure as the active sites, resulting in a MPD 93% of that with Pt/C.[139]

The information on the stability and cost of the metal–AC catalysts in MFCs is limited. The Fe–EDTA/AC cathode with a Fe–EDTA-to-AC ratio of 0.2 : 1 did not show an appreciable change in the MPD after 4.5 months of operation, whereas the Fe–EDTA/AC cathodes with higher ratios degenerated as the Pt/C cathode did,[139] which could be an implication that the structural change by pyrolysis might adversely affect the catalyst durability. In order to better understand the application niches of metal–AC hybrids, future work should focus on the long-term performance and biofouling in real wastewater.

5.2 Metal–CNTs

The feasibility of CNTs as an alternative support of Pt for MFC applications has been demonstrated using sonication or a simple mixing method.[140,141] In addition, *in situ* reduction of Pt salts on the CNT surface could reduce Pt loading and slightly increase the MPD compared to Pt/C.[142] The Pt loading on the CNT textile by electrochemical deposition was further reduced to one fifth of that on a carbon cloth, but the CNT-textile–Pt cathode achieved twice higher MPD than the carbon cloth–Pt cathode.[143] The distinction of CNT–Pt from commercial Pt/C lies in the porous structure of the CNT-textile and the facilitated mass transfer of oxygen to the catalysts (Fig. 8).

As discussed previously, MnO_2 is a promising non-precious metal catalyst and has been hybridized with CNTs in several studies. When mixed with CNTs using sonication, β-MnO_2 outperformed α-MnO_2 and γ-MnO_2 in terms of power production, but was slightly inferior to Pt/C.[144] Hydrothermal reduction of $KMnO_4$ on CNTs achieved a MPD much higher than physical mixing and comparable to that with Pt/C.[145] In another study, coating CNTs with PPy doubled the conductivity of the Mn–CNT composites.[146] Furthermore, treating the CNTs with acid could introduce functional groups that might serve as the additional actives sites in the MnO_2–CNT hybrids.[147] It was observed that both the MPD and electron transfer number were systematically improved with increased MnO_2 content in the CNTs, which could be easily tuned by varying the initial $KMnO_4$ concentration.[148] The MPD of the

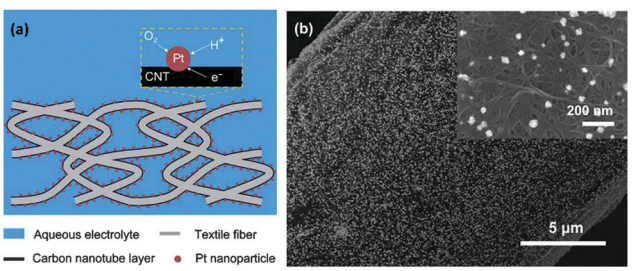

Fig. 8 (a) Schematic of the CNT-textile–Pt composite in aqueous electrolyte and (b) SEM image of the CNT-textile–Pt showing the uniform distribution of Pt nanoparticles. Reproduction with permission from ref. 143. Copyright (2011) The Royal Society of Chemistry.

MnO_2–CNT hybrids exceeded that of the control Pt/C when the MnO_2 content was higher than 60%.

An *in situ* reduction method was also used to hybridize cobalt oxides or nickel oxides in CNTs, usually followed by calcination at 400–500 °C.[149,150] The power production of the Co_3O_4–CNT cathode remained stable in 16 cycles. Meanwhile, the cost of NiO–CNTs was estimated to be \$0.3 g^{-1}, leading to a normalized MPD of 45 mW $\$^{-1}$. The CNFs dispersed with alumina–nickel and doped with nitrogen could achieve an MPD of up to 1850 mW m^{-2},[151,152] but the complicated synthesis, which was composed of impregnating, calcination, reduction and chemical vapor deposition, may not be suitable for mass production. In addition, the long-term stability of these novel metal–CNT catalysts has not been demonstrated yet.

5.3 Metal–graphite/graphene

As previously mentioned, both pristine graphite and graphene do not possess defects in the carbon structures and thus are not catalytically active. Thermal deposition of $Fe(CO)_5$ on graphite felt could introduce Fe_2O_3 and FeOOH as the active sites, and thereby achieving a high MPD comparable to that with Pt/C.[153] To closely incorporate iron in carbon, cornstalks or pomelo skins were impregnated with an $FeCl_3$ solution and graphitized at 1000 °C.[154] The resulting iron oxide/partly graphitized carbon composite showed the lowest ohmic and charge transfer resistance in comparison with bare partly graphitized carbon and Pt/C, and consequently produced the highest MPD. Later, Ag^+ and Fe^{3+} were used for impregnation to form dual-metal modified graphitic carbon composites.[155] Both the Ag nanoparticles and the Fe_3O_4 acted as the active sites, exhibiting a $4e^-$ ORR pathway. In a recent work graphitic carbon was synthesized from a PANI precursor, and the dual active centers were replaced with N-doped carbon and cobalt sulfide.[156] The multi-crystalline Co/Co_9S_8 heterojunction formed at high temperature, together with the nitrogen species originating from the PANI precursor, was speculated to contribute to the improved ORR kinetics and cathode performance.

Graphene has been demonstrated to be an effective support material for metal catalysts such as Pt–Pd and MnO_2.[157,158] *In situ* reduction of MnO_2 on graphene using a microwave method significantly increased the MPD from 1470 mW m^{-2} (pure MnO_2) to 2083 mW m^{-2}, which was also 22% higher than that with Pt/C.[159] It is worth noting that the MnO_2 hydrothermally reduced on graphite oxide, which is considered non-conductive,[76] has achieved a high MPD of 3359 mW m^{-2},[160] and the detailed catalytic mechanisms remain to be studied. The synthesis of metal–graphene catalysts is typically a two-step procedure consisting of the reduction of graphene oxide and the embedding of metals, which may not be practical for MFC applications. To address this issue, SnO_2–graphene catalysts were prepared through microwave-assisted simultaneous reduction of graphite oxide and oxidation of tin salts.[161] A one-step strategy was also adopted to prepare a novel N-doped graphene/CoNi-alloy encased within bamboo-like carbon nanotube hybrids.[162] The CoNi alloy particles were encapsulated at the end of the CNTs, whilst the N-doped graphene filled the inner cavities of the CNTs (Fig. 9). This is the first report that N-doped graphene acts as the active sites instead of the support to enhance ORR catalysis. Moreover, the MFC equipped with the N–G@CoNi/BCNT produced the same current density as that with Pt/C under alkaline conditions (pH = 10, Fig. 9g), highlighting the attractive synergetic effects of the individual components and their potential in buffer-free MFCs.

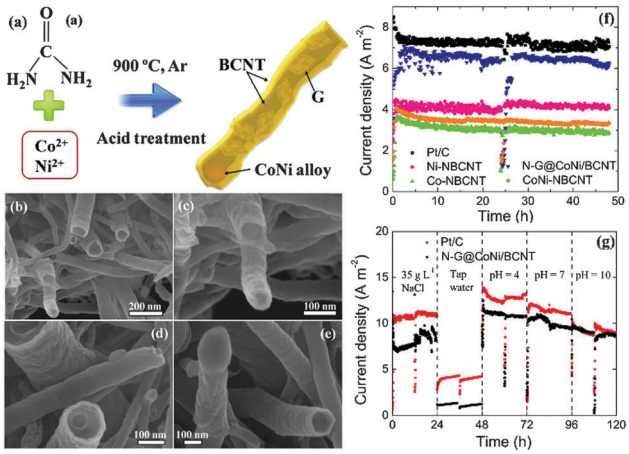

Fig. 9 (a) The synthesis of the N–G@CoNi/BCNT, (b–e) FESEM images of the N–G@CoNi/BCNT at different magnifications, (f) current density of the MFC equipped with different cathode electrodes, and (g) current density of Pt/C and N–G@CoNi/BCNT in different catholytes. Reproduction with permission from ref. 162. Copyright (2016) Elsevier.

Because the transition metals are relatively unstable and graphite/graphene are considered biocompatible,[163,164] the durability of metal–graphite/graphene catalysts will be a critical issue. The power production of the graphitic carbon derived from cornstalks and pomelo skins decreased by 17% and 10% after 18 cycles of operation, respectively, but the decrease was alleviated to 7% by mixing those two types of graphitic carbons.[154] The degeneration was likely attributed to the loose structure and the invasion of biofilms. Replacing the active sites with antibacterial Ag nanoparticles could reduce biofouling and consequently lead to only 4% decrease in the MPD after 17 cycles.[155]

The cost of metal–graphite/graphene catalysts mainly depends on their precursors and synthesis procedures. For instance, the one-step synthesis of N–G@CoNi/BCNTs used 5 g of urea as the carbon and nitrogen source to prepare 1 g of the product (Fig. 9a), whose normalized MPD reached 150 mW $\$^{-1}$.[162] The graphitic carbon produced from renewable resources such as cornstalks or pomelo skins could be even more cost-effective and may meet the requirement of sustainability and economy.

6. Metal–nitrogen–carbon complexes

6.1 Metal macrocycles

Unlike the previously discussed Ni/N–CNFs or N–G@CoNi/BCNTs, in which the metal and nitrogen species do not form chemical bonding, metal–nitrogen–carbon (M–N–C) complexes refer to a wide range of materials with the metal cations coordinated with nitrogen functional groups in carbonaceous matrices.[165]

Metal macrocycles, a class of well-defined M–N–C complexes whose ORR catalytic activity has been studied for fifty years,[166] are among the first alternative cathode catalysts examined in MFCs.[167] The major issue of metal macrocycles is their instability in an acid medium.[168] This is of critical concern particularly for two-chamber MFCs with the anode effluent being further treated in the cathode, where a high concentration of protons is present due to the microbial oxidation of the organic matter (Fig. 1B). Pyrolysis of metal macrocycles at 400–1000 °C can significantly improve both stability and activity, and thus makes them feasible for MFC applications[169]

With the same loading rate of 2 mg cm^{-2}, pyrolyzed iron phthalocyanine (FePc, 700 °C) could achieve a current density comparable to that with Pt/C in the acid medium.[170] Another iron macrocyclic complex, Cl–Fe tetramethoxyphenyl porphyrin, was heat-treated at 800 °C and produced a MPD 80% of that with Pt/C.[171] Although the pyrolyzed iron macrocycles are stable in the acid medium, they still suffer from deterioration under alkaline conditions, which possibly involves deactivation by H_2O_2 generated from the $2e^-$ ORR pathway.[172,173] MnO_x was therefore hybridized with FePc to degrade the accumulated H_2O_2 (Scheme 1), and an improved cathode performance was observed.[174] Whilst the active metal–N center is playing a key role in ORR catalysis, the interaction between the carbon matrix and the carbon support may also affect catalytic kinetics. It has been reported that replacing CB with Ketjen black carbon can increase the power production by 20%.[175] The FePc supported by multi-walled CNTs or PANI, and the iron tetrasulfophthalocyanine mixed with graphene have also shown enhanced MPDs comparable to or even higher than Pt/C.[176–178] A composite of FePc, polyindole and CNTs was obtained without thermal treatment, but showed an electron transfer number of 3.9 and a MPD (799 mW m^{-2}) 1.2 times that with Pt/C,[179] which might be practical for MFC-based wastewater treatment due to the simple fabrication procedures.

The feasibility of Co macrocycles as an alternative cathode catalyst in MFCs was first demonstrated together with FePc a decade ago.[167] Satisfactory MPDs were generated by pyrolyzed cobalt tetramethylphenylporphyrin (CoTMPP) and cobalt naphthalocyanine (~75% relative to that with Pt/C).[180,181] Later, several modifications on cobalt macrocycles were conducted to further promote the catalytic performance. Depositing CoTMPP and FePc on CNTs produced a MPD of 751 mW m^{-2}, 1.5 times that with Pt/C.[182] Cobalt oxide was mixed with cobalt phthalocyanine (CoPc) to serve as the downstream active sites to reduce HO_2^- production and minimize the possible inhibitory effects on the metal–N center.[183] As a consequence, the electron transfer number was increased from ~3.5 to 4 with 20% less production of HO_2^-. The addition of CoO and NiO in non-pyrolyzed binuclear CoPc could increase the MPD by 14% and 23%, respectively.[184] Meanwhile, pyrolyzing binuclear CoPc at different temperatures could increase the nitrogen abundance, particularly that of pyrrolic-N,[185] which might be beneficial for improving the ORR performance.

Both pyrolyzed FePc and CoTMPP were demonstrated to be durable in long-term MFC experiments.[171,180] However, the open circuit potential of FePc distinctly decreased when sulfide was added.[17] This may pose a potential challenge for MFC applications as sulfate in wastewater is readily reduced to sulfide by sulfate-reducing bacteria under anaerobic conditions.[186] Encouragingly, in the same study, FePc was not affected in the presence of various organic metabolites, such as formate, ethanol, lactate and methanol. When exposed to 40 mM methanol, the single-chamber MFC equipped with CoTMPP was not affected, whereas that with Pt/C produced an open circuit potential only half of that in the absence of methanol.[18] The tolerance to the organic matter is of practical relevance for the cathode catalysts in MFCs, as organic matter is constantly added as a carbon source to facilitate power generation.[187]

While technologically promising, metal macrocycles do not seem to be economically feasible for wastewater treatment. The binuclear CoPc-based catalysts were estimated to cost over \$100 m^{-2},[184,185] making the normalized MPD only 4–6 mW $\$^{-1}$. The normalized MPD was increased to 11 mW $\$^{-1}$ using the CoO–FePc mixture,[188] but was still not competitive with carbon-based catalysts.

6.2 M–N–C complexes synthesized from other precursors

During heat treatment, the atomic configuration of metal macrocycles is likely to decompose and form core–shell or substrate–anchor structures, which has been suggested to be the actual active sites of ORR catalysis.[165] It was therefore proposed and verified that precursors other than metal macrocycles could be used to form the metal–N_x/C active sites.[189] Since then, many efforts have been made to construct M–N–C catalysts from a variety of precursors, including polymers, simple organic compounds and metal–organic frameworks (MOFs).

The typical synthesis procedures with polymers start from the polymerization of monomers followed by coordination with metal salts and the final pyrolysis. For example, poly(2,6-diaminopyridine) (PDAP) was impregnated with Co and Fe salts and pyrolyzed under an NH_3 atmosphere at 700 °C (Fig. 10).[190] The obtained products showed an electron transfer number of 3.96, and a MPD (1.2 W m^{-2}) 2.2 times that with Pt/C. The results suggested that the abundance of the Fe–N_x and Co–N_x structures exerted strong influence on ORR catalysis. Similar power production was obtained when melamine-formaldehyde resin (MFR) was used as the precursor and the same procedures were followed.[191] The polymerization step could also be performed after mixing the monomers with the metal salts.[192] Regardless of the synthesis procedures, the pyrolysis temperature is considered the major factor that affects the structure and the consequent catalytic activity. The electron transfer number of a Fe–N–C catalyst increased from 3.48 to 3.86 when the temperature was increased from 800 °C to 900 °C, but

$$2(O_2 + 2e^- + 2H^+) \xrightarrow{\text{FePc /Quinone}} 2H_2O_2 \xrightarrow{Mn_x/C} O_2 + 2H_2O$$

Scheme 1 Reaction scheme for synergetic ORR catalysis by FePc and Mn. Reproduction with permission from ref. 174.

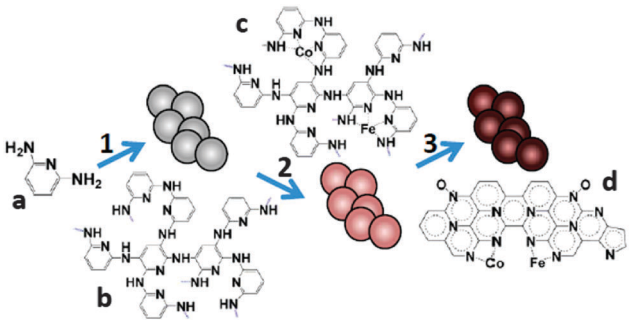

Fig. 10 The synthesis of Co/Fe–PDAP: (1) polymerization, (2) metal coordination and (3) pyrolysis. Reproduction with permission from ref. 190. Copyright (2012) American Chemical Society.

decreased to 3.69 when it was further increased to 1000 °C.[193] The M–N–C complex derived from PANI at 700 °C and 900 °C showed different BET surface areas and varied content of N species, which might explain the different cathode performances.[194]

The strategy using simple organic compounds as the precursor also involves multi-step synthesis and high temperature treatment. For the preparation of Fe- and N-functionalized graphene, graphite oxide was first chemically reduced at 100 °C in the presence of $FeCl_3$ and graphitic C_3N_4, dried at 130 °C and finally pyrolyzed at 800 °C.[195] Although the Fe–N–graphene showed the same onset potential as Pt/C and produced a MPD (1149.8 mW m^{-2}) 2.1 times that with Pt/C, the complicated synthesis may not be applicable for large-scale wastewater treatment. To simplify the procedures, $FeCl_3$ was directly pyrolyzed with cyanamide to form core–shell structured Fe–N–C nanorods, leading to a MPD of 4.3 W m^{-3}, slightly higher than that with Pt/C.[29] $FeCl_3$ was also pyrolyzed with other nitrogen-containing organic compounds such as melamine and ethylenediamine, and the MPDs produced by those Fe–N–C catalysts were both higher than that by Pt/C.[196,197] A recent study prepared Fe–N–C complexes using mebendazole and aminoantipyrine as precursors and observed an attractive phenomenon: the power density of the MFCs equipped with those two catalysts increased when the catholyte pH was increased from 7 to 11.[198] While the detailed catalysis mechanisms remain to be understood, the effective ORR catalysis at high pH is favorable for MFC applications as it can reduce the cost of buffer solutions.

MOFs are highly defined 3D-structured materials composed of metal centers and organic ligands. Owing to the high BET surface area (theoretically up to 10 000 m^2 g^{-1}), uniform open cavities and tunable microstructures, MOFs have gained growing interest in a variety of applications.[199] The abundant M–N–C sites have also made MOFs an ideal candidate for ORR catalysis. There have been a few pioneering studies using MOFs as the precursor to synthesize ORR catalysts in the past five years.[200–204] The application of MOF-based ORR catalysts in MFCs has been reported by two recent studies. Pyrolyzing a Co-MOF (ZIF-67) in the presence of $NiCl_2$ at 800 °C resulted in the formation of N species, Co–N bonding and Ni species in the composite.[205] On the other hand, the BET surface area was reduced from 555 m^2 g^{-1} for the precursor Co-MOF to 194 m^2 g^{-1} for the Ni/Co-MOF. Due to the synergetic effects, the Ni/Co-MOF showed an onset potential more positive than Pt/C, indicating higher ORR catalytic activity. Subsequently, the MFC equipped with the Ni/Co-MOF produced a high MPD of 4336 mW m^{-2}, 1.7 times that with Pt/C. The direct pyrolysis of the same Co-MOF could also yield high catalytic performance, which could be tuned by the heat treatment temperature.[28] It was observed that increasing the pyrolysis temperature could systematically change the BET surface area, shift the pore size distribution and tune the content of carbon and nitrogen.

The configuration change caused by pyrolysis has endowed M–N–C complexes with superior durability.[165] The performance of the Co/Fe–N–C catalysts prepared from polymers such as PDAP and MFR was not affected by methanol crossover,[190,191] and the catalyst from PANI showed only 5% decrease in the MPD after 6 months of operation.[192] In terms of current output, the MFCs equipped with the Fe–N–C nanorods remained unchanged for 6 months when operated with an external resistance of 20 Ω.[29] The study on Fe–AAPyr has delivered more insights into the effects of pollutants.[206] This Fe–AAPyr catalyst generated much more stable electricity than Pt/C in the presence of sulfide and sulfate with concentrations up to 20 mM (Fig. 11). Meanwhile, a thick biofilm was observed on the Fe–AAPyr surface, but did not affect the cathode performance. Biofouling has also been reported to exert a negligible influence on the cathode performance of the pyrolyzed Co-MOF.[28]

The cost effectiveness of M–N–C complexes largely depends on the precursor. Take Fe–AAPyr and Fe–MBZ as examples, the normalized MPD of those catalysts was less than 5 mW $\$^{-1}$ due to the high cost of AAPyr and MBZ ($3.2–3.6 g^{-1}).[198] The price

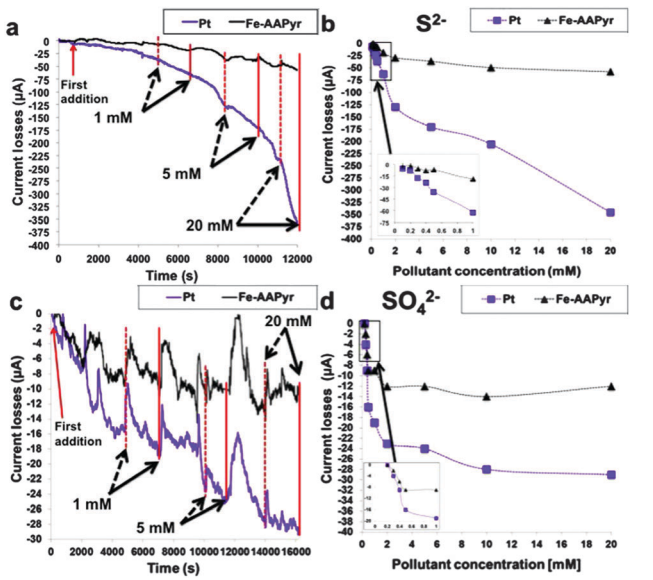

Fig. 11 (a) Chronoamperometry study with the addition of S_2^-, (b) current losses as a function of the S_2^- concentration, (c) chronoamperometry study with the addition of SO_4^{2-} and (d) current losses as a function of SO_4^{2-} concentration. Reproduction with permission from ref. 206. Copyright (2015) Nature Publishing Group.

could be reduced to 5% of that of Pt by using cyanamide as the precursor.[29] Furthermore, the Fe–N–C catalysts obtained from the inexpensive aniline was estimated to cost only \$0.08 g^{-1},[194] making them even competitive to AC-based catalysts.

7. Biocatalysts

Microorganisms can take up electrons from a cathode electrode to reduce oxygen, thereby acting as the ORR catalysts in MFCs.[207] It has been observed that the anode biofilm and several electrochemically active pure cultures (*e.g.*, *Acidithiobacillus ferrooxidans* and *Pseudomonas aeruginosa*) are able to facilitate ORR kinetics.[208–210] Moreover, seven isolates from seawater and one green alga have also been reported to catalyze the ORR,[211,212] indicating that extracellular electron uptake is a common strategy for aerobic respiration. Fundamental studies have suggested that the electron transfer of the microbes on biocathodes involves one or multiple pathways that are commonly found in exoelectrogens.[12,213,214]

The uniqueness of biocatalysts is that the catalytic efficiency is not only determined by the activity of the individual cells, but also affected by the microbial interactions in the community. For instance, the power density produced by the MFCs with pure-culture biocathodes was an order of magnitude lower than that with mixed culture,[215] a phenomenon consistently observed in the studies on the MFC anode.[216] The better performance could be ascribed to the mutualistic interactions between electrochemically active microorganisms and other organisms during metabolism and respiration.[217–219] An example of such mutualism is the integrated algae-MFC, in which the algae provide dissolved oxygen, and the ORR in return buffers the pH of the algal growth medium (*i.e.*, catholyte).[220,221] The synergetic cooperation of algae and biocathodes is of particular interest in sustainable wastewater treatment, as it can further polish the anode effluent by the removal of nitrogen and phosphate and can simultaneously produce electricity and algal biomass as energy.

The fact that the microorganisms in the MFC anodes and biocathodes share similar electron transfer pathways implies that the features of an effective anode electrode, such as good biocompatibility, high surface area and high conductivity,[14] should be considered when developing the electrodes of biocathodes. Several carbon materials, including graphite, activated carbon and semicoke were examined as the support of biocathodes and produced satisfactory power densities of up to 100 W m^{-3} or 700 mW m^{-2}.[222–226] Modifying carbon materials with conductive polymers could introduce functional groups that help alleviate the change in dissolved oxygen and pH, and encourage biofilm attachment, both of which could improve the cathode performance.[227,228] Nano-structured carbon materials such as CNTs and graphene with a high surface area and high conductivity have also been shown to facilitate the electron transfer of biocathodes.[229–231]

In addition to microorganisms, redox active enzymes have also been used in MFC cathodes as the biocatalysts. Laccase is a copper containing oxidoreductase that can effectively catalyse the ORR with the assistance of redox mediators (*e.g.*, (2,2′-azino-bis(3-ethylbenzo-thiazoline-6-sulfonic acid)diammonium salt)).[232,233] Immobilizing laccase on an air-breathing cathode could avoid the use of the mediator and enhance the mass transfer.[234] To further overcome the limitations caused by enzyme purification, white-rot fungus was inoculated in the cathode to directly excrete laccase for ORR catalysis.[235] Another enzyme, bilirubin oxidase, was immobilized on a yeast surface or immobilized on an air cathode and was proved to be feasible as the cathode catalyst.[236,237]

In terms of cost, microorganisms and enzymes excreted by yeast or fungi may be ideal ORR catalysts for MFC applications. The cathode ORR catalysts can affect wastewater treatment efficiency through current generation, which can stimulate the removal of organic contaminants. Moreover, biocatalysts can be used to remove the excess organic matters from the anode effluent, thereby producing high-quality water and further enhancing the cost effectiveness of wastewater treatment. With different carbon materials as the support, the COD removal by biocatalysts could reach up to 90%.[225,226] Biocatalysts could also facilitate the removal of toxic and refractory pollutants such as *p*-nitrophenol (PNP).[238] The MFC biocathode removed 100% of the PNP in 50 h, while the abiotic cathode achieved only 70.2% removal. The enzymatic cathode with immobilized laccase has been reported to simultaneously generate power and decolorize azo dye, a primary pollutant in industrial wastewater that affects the clarity and oxygen solubility.[239]

Biocatalysts suffer from stability issues, which are largely attributed to the microbial community dynamics. It has been reported that the biocathode with the potential fixed at 250 mV *vs.* Ag/AgCl, at which MPD is typically obtained, shows a long start-up period and negligible current generation.[240] Further experiments using phylogenetic analysis revealed that the biocathode poised at higher potential had a higher diversity, indicating a stronger competition between the electrochemically active microorganisms and other organisms.[241] The heterotrophs are likely to outcompete the biocathode community for oxygen, leading to decreased power production after long-term operation.[242] For the enzyme-based MFCs, bilirubin oxidase was immediately deactivated in wastewater. The restoration of the catalytic activity of biocatalysts may be more difficult than that of abiotic catalysts, as the non-functional biofilm needs to be removed and the time-consuming acclimation needs again to be performed. Hence, the application of biocatalysts requires advances in engineering to maintain a stable environment for the organisms and enzymes.

8. Perspectives

The goal of MFC development is to achieve energy-efficient wastewater treatment, and accordingly the ideal cathode catalysts should be simple to synthesize, durable after long-term operation, stable in wastewater and cost-effective (Table 1). In this regard, carbon-based catalysts, particularly N-doped AC, may be the most promising candidate for practical applications.

Table 1 The synthesis/modification, stability and cost effectiveness of representative ORR catalysts from each category

	Category	Catalysts/synthesis	n^a	MPD[b]	Stability	Cost effectiveness	Ref.
Carbon-based catalysts	Carbon black	Polypyrrole/carbon black composite		401.8 mW m^{-2}	Biofilm formation	15 times that with Pt/C	35
	Activated carbon	Activated carbon/carbon black mixture		1210 mW m^{-2}	15% decrease in MPD after 16 months	1210 mW $\$^{-1}$	53
	Carbon nanofibers	Alkaline treatment		61.3 mW m^{-2}		2.6 times that with Pt/C	60
	Carbon nanotubes	Polyaniline/multi-walled CNTs composite		488 mW m^{-2}		31 mW $\$^{-1}$	71
	Graphene	N/S co-doped carbon nanosheets	3.5	1.5 W m^{-2}	Stable after 6000 cycles of CV	10 mW $\$^{-1}$	84
	Carbon-based catalysts synthesized from biochar, cellulose, dopamine, straw, chitin, petroleum coke and moss		3.5	2293 mW m^{-2}	Stable in long-term experiments, tolerant to crossover	>143 mW $\$^{-1}$ (free precursors)	95
Metal-based catalysts	Platinum	Electron beam evaporation				Reduced Pt loading	104
	Silver nanoparticles				Inhibit bacterial growth		110
	Perovskite oxides			405 mW m^{-2}	15% decrease in MPD after 15 cycles	116 mW $\$^{-1}$	125
Metal–carbon hybrids	Metal–AC	Pyrolysis of Fe–EDTA and AC		1580 mW m^{-2}	No change in MPD after 4.5 months		139
	Metal–CNT	NiO/CNT with *in situ* reduction and calcination	3.5	670 mW m^{-2}		45 mW $\$^{-1}$	149
	Metal–graphite	Carbonized AgNPs/Fe_3O_4/GC	3.98	1712 mW m^{-2}	Inhibit bacterial growth		155
	Metal–graphene	N-Doped graphene/CoNi alloy encased within bamboo-like CNT	3.63	2.0 mW m^{-2}		150 mW $\$^{-1}$	162
Metal–nitrogen–carbon complexes	Metalmacrocycles	CoO–FePc mixture		654 mW m^{-2}	85% decrease in MPD after 60 days	11 mW $\$^{-1}$	188
	N–Fe/Fe_3C@C	Pyrolysis of cyanamide and $FeCl_3$	3.98	4.2 W m^{-3}	Stable current output over 6 months	5% of that of Pt	29
Biocatalysts	Microorganisms	Mixed culture		554 mW m^{-2}	64% decrease in MPD after 9 cycles	Free	242
	Enzymes	Laccase		26 W m^{-3}	4% loss in potential after 5 days		234

[a] n, electron transfer number. [b] MPD, maximum power density.

The normalized MPD of 1210 mW $\$^{-1}$ achieved by the AC mixed with CB is by far the highest reported in the literature. Further studies are needed to understand the roles of AC precursors, elucidate the mechanisms of heteroatom doping and develop a simple treatment for mass production. Metal-based catalysts do not seem competitive compared with carbon materials in terms of durability and cost, but the hybridization of metal and carbon can combine the advantages of the individual components and thus greatly enhance catalytic performance. M–N–C complexes present a new group of catalysts with excellent catalytic activity and high stability, and are particularly attractive with the effective ORR catalysis under alkaline conditions. Finally, biocatalysts are sustainable and free, but the resilience towards fluctuation remains to be improved.

One of the advantages of biocatalysts over abiotic catalysts is the additional treatment of wastewater by microbes. However, recent studies have demonstrated that integrated catalyst-membrane assembly can also produce effluent with high quality.[243] Coating multiwalled CNTs on nonwoven polyester formed an ultrafiltration membrane with a pore size of $\sim$65 nm that could simultaneously produce energy and filtrate wastewater in a single-chamber MFC.[244] The MFC using the membrane modified with a C–Mn–Fe–O catalyst could remove up to 90% COD and 80% NH_4^+–N.[245] In addition to the good performance, the integration of ORR catalysts with membranes can improve system stability. Fouling mitigation was observed when the membrane was coated with different catalysts,[246,247] possibly because the electric field reduced the deposition of sludge on the membrane surface, and the H_2O_2 produced by the cathode removed the foulants.[248] With stable energy and water production, catalyst–membrane assembly may be more cost-effective than individual MFCs and membrane bioreactors. It was estimated that the cathode membrane prepared from carbon foam and transition metals cost only 10% of the total price of Pt/C and commercial filtration membranes.[249] Such a combination may provide a new direction in the study of abiotic ORR catalysts for MFC-based wastewater treatment.

Regardless of the catalyst materials, biofouling is almost inevitable when the cathode electrode is exposed to wastewater. The inefficient ORR catalysis, *i.e.*, the $2e^-$ pathway with the production of H_2O_2, may provide a solution for the fouling issue. Most of the ORR catalysts discussed in this review produce a considerable amount of H_2O_2 under normal MFC operation. For example, at the MPD, C–CoPc generated a current density of 2.5 A m^{-2} (green triangle, Fig. 12A) and the corresponding cathode potential of -0.2 V *vs.* SCE (Fig. 12B). The electron transfer number at this cathode potential was measured to be 3, with 50% of the ORR product being hydrogen peroxide ions (Fig. 12C).[183] The high H_2O_2 production, as discussed in the catalyst–membrane assembly, may contribute to fouling mitigation. The study using graphite particles as the cathode electrode could produce 196.5 mg L^{-1} H_2O_2 in 24 h, but did not further investigate the effects on fouling.[250] Therefore, the relation between H_2O_2 production and biofilm formation can be a focus for future research.

Depending on the pH conditions, the overall equation of ORR can either be proton consuming (acid medium) or hydroxide producing (alkaline medium).[47] Experiments and modeling suggest that the ORR in the neutral catholyte proceeds dominantly *via* the OH^--producing pathway.[251] The OH^- accumulated at the catalytic sites could lead to a potential loss over 0.3 V at high current density. Such a potential loss may explain the finding that power density negatively correlates with the micropore volume of the AC.[39] The small pore hinders OH^- transportation, thereby resulting in large concentration overpotential. Moreover, the commonly used Nafion binder, which was not anion-conducting, was speculated to further contribute to OH^- build-up.[251] The functional groups on the catalyst surface may act in a similar way and significantly affect the OH^- transportation and ORR kinetics. In addition to potential loss, the elevated pH may affect the stability of the catalysts. For example, iron macrocycles lose catalytic activity under alkaline conditions.[173] The effects of high pH on the stability of other catalysts is of practical significance and thus warrant further studies.

The development of ORR catalysts can greatly benefit bioelectrochemical systems (BES) other than MFCs, such as microbial desalination cells (MDCs) and microbial electrolysis cells (MECs). MDCs also use oxygen as the cathode electron acceptor and can achieve simultaneous wastewater treatment and desalination at low energy consumption.[252,253] While the unit price of the ORR catalysts in MDCs remains the same as in MFCs, the

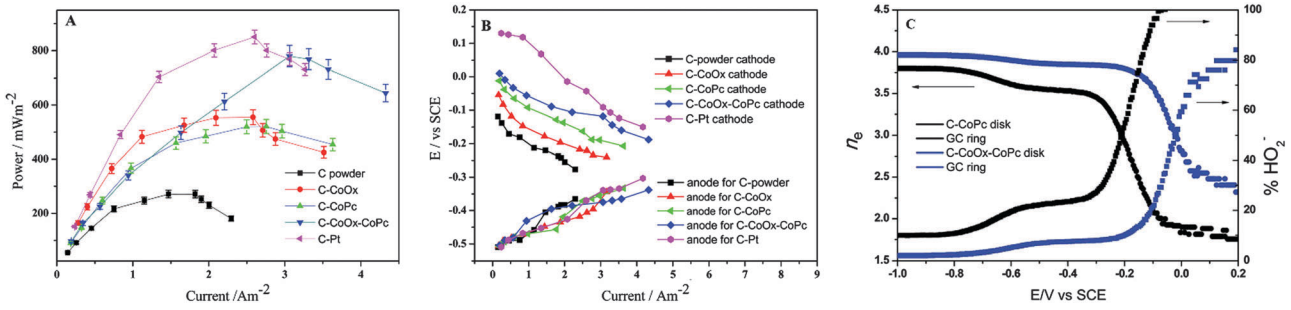

Fig. 12 (A) Plot of power density *vs.* current density for MFCs constructed with carbon power, C–CoOx, C–CoPc, C–CoOx–CoPc and C–Pt; (B) individual electrode potential measured with respect to SCE as a function of current density and (C) plots of the number of electrons transferred (left) and the percent yield of hydrogen peroxide (right) during the oxygen reduction as a function of potential. Reproduction with permission from ref. 183. Copyright (2014) The Royal Society of Chemistry.

cost effectiveness may be significantly increased when fresh water production and net energy balance are considered. MECs can produce hydrogen gas by using protons as the electron acceptor.[254,255] Similar to ORR, hydrogen evolution reaction (HER) is sluggish and needs the presence of catalysts.[256,257] Multi-functional catalysts for ORR, OER (oxygen evolution reaction) and HER have recently been reported,[258–262] which can make BES a more versatile technology that can be easily switched between MFCs and MECs to meet the special requirement of applications. It can be expected that ORR catalysts will play an important role in energy-efficient water and wastewater treatment in the future, and there will be an increasing need for identifying their appropriate application niches.

Acknowledgements

This work was made possible by NPRP grant # 6-289-2-125 from the Qatar National Research Fund (a member of Qatar Foundation). The statements made herein are solely the responsibility of the authors.

Notes and references

1 WWAP (United Nations World Water Assessment Programme), *The United Nations World Water Development Report 2014: Water and Energy*, Paris, UNESCO, 2014, ISBN 978-92-3-104259-1.
2 R. Goldstein and W. Smith, *Water & Sustainability, US Electricity Consumption for Water Supply & Treatment-The Next Half Century*, Electric Power Research Institute, vol. 4, 2002.
3 P. L. McCarty, J. Bae and J. Kim, *Environ. Sci. Technol.*, 2011, **45**, 7100–7106.
4 A. L. Smith, S. J. Skerlos and L. Raskin, *Water Res.*, 2013, **47**, 1655–1665.
5 B. E. Logan, B. Hamelers, R. Rozendal, U. Schröder, J. Keller, S. Freguia, P. Aelterman, W. Verstraete and K. Rabaey, *Environ. Sci. Technol.*, 2006, **40**, 5181–5192.
6 D. R. Lovley, *Annu. Rev. Microbiol.*, 2012, **66**, 391–409.
7 W.-W. Li, H.-Q. Yu and Z. He, *Energy Environ. Sci.*, 2014, **7**, 911–924.
8 B. E. Logan, *Appl. Microbiol. Biotechnol.*, 2010, **85**, 1665–1671.
9 Y. Fan, E. Sharbrough and H. Liu, *Environ. Sci. Technol.*, 2008, **42**, 8101–8107.
10 R. A. Rozendal, H. V. Hamelers, K. Rabaey, J. Keller and C. J. Buisman, *Trends Biotechnol.*, 2008, **26**, 450–459.
11 Z. Wang, C. Cao, Y. Zheng, S. Chen and F. Zhao, *ChemElectroChem*, 2014, **1**, 1813–1821.
12 X.-W. Liu, W.-W. Li and H.-Q. Yu, *Chem. Soc. Rev.*, 2014, **43**, 7718–7745.
13 K. Ben Liew, W. R. W. Daud, M. Ghasemi, J. X. Leong, S. Su Lim and M. Ismail, *Int. J. Hydrogen Energy*, 2014, **39**, 4870–4883.
14 H. Yuan and Z. He, *Nanoscale*, 2015, **7**, 7022–7029.
15 Z. Ge, J. Li, L. Xiao, Y. Tong and Z. He, *Environ. Sci. Technol. Lett.*, 2014, **1**, 137–141.
16 T. Schmidt, U. Paulus, H. Gasteiger and R. Behm, *J. Electroanal. Chem.*, 2001, **508**, 41–47.
17 F. Harnisch, S. Wirth and U. Schröder, *Electrochem. Commun.*, 2009, **11**, 2253–2256.
18 B. Liu, C. Brückner, Y. Lei, Y. Cheng, C. Santoro and B. Li, *J. Power Sources*, 2014, **257**, 246–253.
19 P. D. Kiely, G. Rader, J. M. Regan and B. E. Logan, *Bioresour. Technol.*, 2011, **102**, 361–366.
20 Y. Yuan, S. Zhou and J. Tang, *Environ. Sci. Technol.*, 2013, **47**, 4911–4917.
21 Z. He and L. T. Angenent, *Electroanalysis*, 2006, **18**, 2009–2015.
22 F. Zhang, Z. Ge, J. Grimaud, J. Hurst and Z. He, *Environ. Sci. Technol.*, 2013, **47**, 4941–4948.
23 S. Jung and J. M. Regan, *Appl. Environ. Microbiol.*, 2011, **77**, 564–571.
24 Z. He and F. Mansfeld, *Energy Environ. Sci.*, 2009, **2**, 215.
25 F. Zhao, R. C. Slade and J. R. Varcoe, *Chem. Soc. Rev.*, 2009, **38**, 1926–1939.
26 Y. Feng, X. Shi, X. Wang, H. Lee, J. Liu, Y. Qu, W. He, S. M. S. Kumar, B. H. Kim and N. Ren, *Biosens. Bioelectron.*, 2012, **35**, 413–415.
27 X.-B. Gong, S.-J. You, X.-H. Wang, Y. Gan, R.-N. Zhang and N.-Q. Ren, *J. Power Sources*, 2013, **225**, 330–337.
28 S. You, X. Gong, W. Wang, D. Qi, X. Wang, X. Chen and N. Ren, *Adv. Energy Mater.*, 2016, **6**, DOI: 10.1002/aenm.201501497.
29 Z. Wen, S. Ci, F. Zhang, X. Feng, S. Cui, S. Mao, S. Luo, Z. He and J. Chen, *Adv. Mater.*, 2012, **24**, 1399–1404.
30 J.-B. Donnet, *Carbon black: science and technology*, CRC Press, 1993.
31 *PEM fuel cell electrocatalysts and catalyst layers: fundamentals and applications*, ed. J. Zhang, Springer Science & Business Media, 2008.
32 N. Duteanu, B. Erable, S. M. Senthil Kumar, M. M. Ghangrekar and K. Scott, *Bioresour. Technol.*, 2010, **101**, 5250–5255.
33 G. Yang, Y. Sun, Z. Yuan, P. Lü, X. Kong, L. Li, G. Chen and T. Lu, *Chin. J. Catal.*, 2014, **35**, 770–775.
34 K. Meng, Q. Liu, Y. Huang and Y. Wang, *J. Mater. Chem. A*, 2015, **3**, 6873–6877.
35 Y. Yuan, S. Zhou and L. Zhuang, *J. Power Sources*, 2010, **195**, 3490–3493.
36 H. Marsh and F. R. Reinoso, *Activated carbon*, Elsevier, 2006.
37 T. Iwazaki, R. Obinata, W. Sugimoto and Y. Takasu, *Electrochem. Commun.*, 2009, **11**, 376–378.
38 F. Zhang, S. Cheng, D. Pant, G. V. Bogaert and B. E. Logan, *Electrochem. Commun.*, 2009, **11**, 2177–2179.
39 V. J. Watson, C. Nieto Delgado and B. E. Logan, *Environ. Sci. Technol.*, 2013, **47**, 6704–6710.
40 A. Janicek, N. Gao, Y. Fan and H. Liu, *Fuel Cells*, 2015, **15**, 855–861.
41 X. Zhang, X. Xia, I. Ivanov, X. Huang and B. E. Logan, *Environ. Sci. Technol.*, 2014, **48**, 2075–2081.
42 X. Wang, N. Gao, Q. Zhou, H. Dong, H. Yu and Y. Feng, *Bioresour. Technol.*, 2013, **144**, 632–636.
43 Z. Chen, K. Li and L. Pu, *Bioresour. Technol.*, 2014, **170**, 379–384.

44 Z. Chen, K. Li, P. Zhang, L. Pu, X. Zhang and Z. Fu, *Chem. Eng. J.*, 2015, **259**, 820–826.
45 Y. Liu, K. Li, Y. Liu, L. Pu, Z. Chen and S. Deng, *J. Mater. Chem. A*, 2015, **3**, 21149–21158.
46 V. J. Watson, C. Nieto Delgado and B. E. Logan, *J. Power Sources*, 2013, **242**, 756–761.
47 L. Dai, Y. Xue, L. Qu, H.-J. Choi and J.-B. Baek, *Chem. Rev.*, 2015, **115**, 4823–4892.
48 L. Lai, J. R. Potts, D. Zhan, L. Wang, C. K. Poh, C. Tang, H. Gong, Z. Shen, J. Lin and R. S. Ruoff, *Energy Environ. Sci.*, 2012, **5**, 7936–7942.
49 H. Wang, T. Maiyalagan and X. Wang, *ACS Catal.*, 2012, **2**, 781–794.
50 B. Zhang, Z. Wen, S. Ci, S. Mao, J. Chen and Z. He, *ACS Appl. Mater. Interfaces*, 2014, **6**, 7464–7470.
51 D. Li, Y. Qu, J. Liu, W. He, H. Wang and Y. Feng, *J. Power Sources*, 2014, **272**, 909–914.
52 N. Li, Y. Liu, J. An, C. Feng and X. Wang, *J. Power Sources*, 2014, **272**, 895–899.
53 X. Zhang, D. Pant, F. Zhang, J. Liu, W. He and B. E. Logan, *ChemElectroChem*, 2014, **1**, 1859–1866.
54 H. Dong, H. Yu and X. Wang, *Environ. Sci. Technol.*, 2012, **46**, 13009–13015.
55 S. Cheng and J. Wu, *Bioelectrochemistry*, 2013, **92**, 22–26.
56 B. Wei, J. C. Tokash, G. Chen, M. A. Hickner and B. E. Logan, *RSC Adv.*, 2012, **2**, 12751–12758.
57 W. Yang, W. He, F. Zhang, M. A. Hickner and B. E. Logan, *Environ. Sci. Technol. Lett.*, 2014, **1**, 416–420.
58 J. Huang, Y. Liu and T. You, *Anal. Methods*, 2010, **2**, 202–211.
59 L. Feng, N. Xie and J. Zhong, *Materials*, 2014, **7**, 3919–3945.
60 M. Ghasemi, S. Shahgaldi, M. Ismail, B. H. Kim, Z. Yaakob and W. R. Wan Daud, *Int. J. Hydrogen Energy*, 2011, **36**, 13746–13752.
61 C. Santoro, A. Stadlhofer, V. Hacker, G. Squadrito, U. Schröder and B. Li, *J. Power Sources*, 2013, **243**, 499–507.
62 S. Chen, Y. Chen, G. He, S. He, U. Schröder and H. Hou, *Biosens. Bioelectron.*, 2012, **34**, 282–285.
63 X. Yang, W. Zou, Y. Su, Y. Zhu, H. Jiang, J. Shen and C. Li, *J. Power Sources*, 2014, **266**, 36–42.
64 L. Zhou, P. Fu, X. Cai, S. Zhou and Y. Yuan, *Appl. Catal., B*, 2016, **188**, 31–38.
65 S. van Dommele, *Nitrogen doped carbon nanotubes: synthesis, characterization and catalysis*, Utrecht University, 2008, ISBN 978-90-6464-263-0.
66 M. F. De Volder, S. H. Tawfick, R. H. Baughman and A. J. Hart, *Science*, 2013, **339**, 535–539.
67 N. Daems, X. Sheng, I. F. J. Vankelecom and P. P. Pescarmona, *J. Mater. Chem. A*, 2014, **2**, 4085–4110.
68 L. Feng, Y. Yan, Y. Chen and L. Wang, *Energy Environ. Sci.*, 2011, **4**, 1892–1899.
69 Y.-R. He, F. Du, Y.-X. Huang, L.-M. Dai, W.-W. Li and H.-Q. Yu, *J. Mater. Chem. A*, 2016, **4**, 1632–1636.
70 K. Gong, F. Du, Z. Xia, M. Durstock and L. Dai, *Science*, 2009, **323**, 760–764.
71 Y. Jiang, Y. Xu, Q. Yang, Y. Chen, S. Zhu and S. Shen, *Int. J. Energy Res.*, 2014, **38**, 1416–1423.
72 M. Ghasemi, W. R. Wan Daud, S. H. A. Hassan, T. Jafary, M. Rahimnejad, A. Ahmad and M. H. Yazdi, *Int. J. Hydrogen Energy*, 2015, **41**, 4872–4878.
73 D. Chung, *J. Mater. Sci.*, 2002, **37**, 1475–1489.
74 K. S. Novoselov, A. K. Geim, S. Morozov, D. Jiang, Y. Zhang, S. Dubonos, I. Grigorieva and A. Firsov, *Science*, 2004, **306**, 666–669.
75 R. S. Edwards and K. S. Coleman, *Nanoscale*, 2013, **5**, 38–51.
76 F. Perreault, A. Fonseca de Faria and M. Elimelech, *Chem. Soc. Rev.*, 2015, **44**, 5861–5896.
77 S. Freguia, K. Rabaey, Z. Yuan and J. Keller, *Electrochim. Acta*, 2007, **53**, 598–603.
78 B. Erable, N. Duteanu, S. M. S. Kumar, Y. Feng, M. M. Ghangrekar and K. Scott, *Electrochem. Commun.*, 2009, **11**, 1547–1549.
79 L. Zhang, Z. Lu, D. Li, J. Ma, P. Song, G. Huang, Y. Liu and L. Cai, *J. Cleaner Prod.*, 2016, **115**, 332–336.
80 X. Shi, Y. Feng, X. Wang, H. Lee, J. Liu, Y. Qu, W. He, S. M. S. Kumar and N. Ren, *Bioresour. Technol.*, 2012, **108**, 89–93.
81 L. Feng, Y. Chen and L. Chen, *ACS Nano*, 2011, **5**, 9611–9618.
82 L. Feng, L. Yang, Z. Huang, J. Luo, M. Li, D. Wang and Y. Chen, *Sci. Rep.*, 2013, **3**, DOI: 10.1038/srep03306.
83 J. Liang, Y. Jiao, M. Jaroniec and S. Z. Qiao, *Angew. Chem., Int. Ed.*, 2012, **51**, 11496–11500.
84 H. Yuan, Y. Hou, Z. Wen, X. Guo, J. Chen and Z. He, *ACS Appl. Mater. Interfaces*, 2015, **7**, 18672–18678.
85 Q. Wen, S. Wang, J. Yan, L. Cong, Y. Chen and H. Xi, *Bioelectrochemistry*, 2014, **95**, 23–28.
86 J. Luo, H. D. Jang, T. Sun, L. Xiao, Z. He, A. P. Katsoulidis, M. G. Kanatzidis, J. M. Gibson and J. Huang, *ACS Nano*, 2011, **5**, 8943–8949.
87 L. Xiao, J. Damien, J. Luo, H. D. Jang, J. Huang and Z. He, *J. Power Sources*, 2012, **208**, 187–192.
88 Y. Liu, H. Liu, C. Wang, S.-X. Hou and N. Yang, *Environ. Sci. Technol.*, 2013, **47**, 13889–13895.
89 C. K. Chua and M. Pumera, *Chem. Soc. Rev.*, 2014, **43**, 291–312.
90 Y.-X. Huang, X.-W. Liu, J.-F. Xie, G.-P. Sheng, G.-Y. Wang, Y.-Y. Zhang, A.-W. Xu and H.-Q. Yu, *Chem. Commun.*, 2011, **47**, 5795–5797.
91 Y.-C. Yong, X.-C. Dong, M. B. Chan-Park, H. Song and P. Chen, *ACS Nano*, 2012, **6**, 2394–2400.
92 Y. Yuan, T. Yuan, D. Wang, J. Tang and S. Zhou, *Bioresour. Technol.*, 2013, **144**, 115–120.
93 Y. Yuan, T. Liu, P. Fu, J. Tang and S. Zhou, *J. Mater. Chem. A*, 2015, **3**, 8475–8482.
94 Q. Liu, S. Chen, Y. Zhou, S. Zheng, H. Hou and F. Zhao, *J. Power Sources*, 2014, **261**, 245–248.
95 Q. Liu, Y. Zhou, S. Chen, Z. Wang, H. Hou and F. Zhao, *J. Power Sources*, 2015, **273**, 1189–1193.
96 G. Yue, K. Meng and Q. Liu, *ChemPlusChem*, 2015, **80**, 1133–1138.
97 S. Zhong, L. Zhou, L. Wu, L. Tang, Q. He and J. Ahmed, *J. Power Sources*, 2014, **272**, 344–350.

98 L. Liu, Q. Xiong, C. Li, Y. Feng and S. Chen, *RSC Adv.*, 2015, **5**, 89771–89776.
99 H. Yuan, L. Deng, X. Cai, S. Zhou, Y. Chen and Y. Yuan, *RSC Adv.*, 2015, **5**, 56121–56129.
100 P. Zhang, X.-H. Liu, K.-X. Li and Y.-R. Lu, *Int. J. Hydrogen Energy*, 2015, **40**, 13530–13537.
101 L. Zhou, P. Fu, D. Wen, Y. Yuan and S. Zhou, *Appl. Catal., B*, 2016, **181**, 635–643.
102 F. H. B. Lima, J. Zhang, M. H. Shao, K. Sasaki, M. B. Vukmirovic, E. A. Ticianelli and R. R. Adzic, *J. Phys. Chem. C*, 2007, **111**, 404–410.
103 V. P. Zhdanov and B. Kasemo, *Electrochem. Commun.*, 2006, **8**, 1132–1136.
104 H. I. Park, U. Mushtaq, D. Perello, I. Lee, S. K. Cho, A. Star and M. Yun, *Energy Fuels*, 2007, **21**, 2984–2990.
105 J.-N. Zhang, S.-J. You, Y.-X. Yuan, Q.-L. Zhao and G.-D. Zhang, *Electrochem. Commun.*, 2011, **13**, 903–905.
106 Y.-Y. Chang, H.-Z. Zhao, C. Zhong and A. Xue, *Russ. J. Electrochem.*, 2014, **50**, 885–890.
107 J. K. Nørskov, J. Rossmeisl, A. Logadottir, L. Lindqvist, J. R. Kitchin, T. Bligaard and H. Jónsson, *J. Phys. Chem. B*, 2004, **108**, 17886–17892.
108 Z. Yan, M. Wang, Y. Lu, R. Liu and J. Zhao, *J. Solid State Electrochem.*, 2013, **18**, 1087–1097.
109 Z. Yan, M. Wang, J. Liu, R. Liu and J. Zhao, *Electrochim. Acta*, 2014, **141**, 331–339.
110 J. An, H. Jeon, J. Lee and I. S. Chang, *Environ. Sci. Technol.*, 2011, **45**, 5441–5446.
111 O. Lefebvre, Z. Tan, Y. Shen and H. Y. Ng, *Bioresour. Technol.*, 2013, **127**, 158–164.
112 M. M. Thackeray, M. H. Rossouw, A. de Kock, A. P. de la Harpe, R. J. Gummow, K. Pearce and D. C. Liles, *J. Power Sources*, 1993, **43**, 289–300.
113 I. Roche, K. Katuri and K. Scott, *J. Appl. Electrochem.*, 2009, **40**, 13–21.
114 L. Zhang, C. Liu, L. Zhuang, W. Li, S. Zhou and J. Zhang, *Biosens. Bioelectron.*, 2009, **24**, 2825–2829.
115 X. Li, B. Hu, S. Suib, Y. Lei and B. Li, *J. Power Sources*, 2010, **195**, 2586–2591.
116 K. A. Stoerzinger, M. Risch, B. Han and Y. Shao-Horn, *ACS Catal.*, 2015, **5**, 6021–6031.
117 X.-W. Liu, X.-F. Sun, Y.-X. Huang, G.-P. Sheng, K. Zhou, R. J. Zeng, F. Dong, S.-G. Wang, A.-W. Xu, Z.-H. Tong and H.-Q. Yu, *Water Res.*, 2010, **44**, 5298–5305.
118 J.-Y. Liao, D. Higgins, G. Lui, V. Chabot, X. Xiao and Z. Chen, *Nano Lett.*, 2013, **13**, 5467–5473.
119 H. Yuan, L. Deng, J. Tang, S. Zhou, Y. Chen and Y. Yuan, *ChemElectroChem*, 2015, **2**, 1152–1158.
120 F. Cheng, J. Shen, B. Peng, Y. Pan, Z. Tao and J. Chen, *Nat. Chem.*, 2011, **3**, 79–84.
121 S. Khilari, S. Pandit, D. Das and D. Pradhan, *Biosens. Bioelectron.*, 2014, **54**, 534–540.
122 D. Hu, H. Wang, J. Wang and Q. Zhong, *Energy Technol.*, 2015, **3**, 48–54.
123 S. Khilari, S. Pandit, J. L. Varanasi, D. Das and D. Pradhan, *ACS Appl. Mater. Interfaces*, 2015, **7**, 20657–20666.
124 J. M. Morris, S. Jin, J. Wang, C. Zhu and M. A. Urynowicz, *Electrochem. Commun.*, 2007, **9**, 1730–1734.
125 H. Dong, H. Yu, X. Wang, Q. Zhou and J. Sun, *J. Chem. Technol. Biotechnol.*, 2013, **88**, 774–778.
126 K. B. Ghoreishi, M. Ghasemi, M. Rahimnejad, M. A. Yarmo, W. R. W. Daud, N. Asim and M. Ismail, *Int. J. Energy Res.*, 2014, **38**, 70–77.
127 M. T. Noori, M. M. Ghangrekar and C. K. Mukherjee, *Int. J. Hydrogen Energy*, 2016, **41**, 3638–3645.
128 X.-B. Gong, S.-J. You, X.-H. Wang, J.-N. Zhang, Y. Gan and N.-Q. Ren, *Biosens. Bioelectron.*, 2014, **55**, 237–241.
129 B. Mecheri, A. Iannaci, A. D'Epifanio, A. Mauri and S. Licoccia, *ChemPlusChem*, 2016, **81**, 80–85.
130 I. Singh and A. Chandra, *Bioresour. Technol.*, 2013, **142**, 77–81.
131 I. Singh and A. Chandra, *Int. J. Hydrogen Energy*, 2016, **41**, 1913–1920.
132 B. Ge, K. Li, Z. Fu, L. Pu and X. Zhang, *Bioresour. Technol.*, 2015, **195**, 180–187.
133 B. Ge, K. Li, Z. Fu, L. Pu, X. Zhang, Z. Liu and K. Huang, *J. Power Sources*, 2016, **303**, 325–332.
134 Z. Fu, L. Yan, K. Li, B. Ge, L. Pu and X. Zhang, *Biosens. Bioelectron.*, 2015, **74**, 989–995.
135 P. Zhang, K. Li and X. Liu, *J. Power Sources*, 2014, **264**, 248–253.
136 L. Pu, K. Li, Z. Chen, P. Zhang, X. Zhang and Z. Fu, *J. Power Sources*, 2014, **268**, 476–481.
137 Z. Liu, K. Li, X. Zhang, B. Ge and L. Pu, *Bioresour. Technol.*, 2015, **195**, 154–161.
138 X. Zhang, K. Li, P. Yan, Z. Liu and L. Pu, *Bioresour. Technol.*, 2015, **187**, 299–304.
139 X. Xia, F. Zhang, X. Zhang, P. Liang, X. Huang and B. E. Logan, *ACS Appl. Mater. Interfaces*, 2013, **5**, 7862–7866.
140 D. V. Sanchez, P. Huynh, M. E. Kozlov, R. H. Baughman, R. D. Vidic and M. Yun, *Energy Fuels*, 2010, **24**, 5897–5902.
141 H. Wang, Z. Wu, A. Plaseied, P. Jenkins, L. Simpson, C. Engtrakul and Z. Ren, *J. Power Sources*, 2011, **196**, 7465–7469.
142 M. Ghasemi, M. Ismail, S. K. Kamarudin, K. Saeedfar, W. R. W. Daud, S. H. A. Hassan, L. Y. Heng, J. Alam and S.-E. Oh, *Appl. Energy*, 2013, **102**, 1050–1056.
143 X. Xie, M. Pasta, L. Hu, Y. Yang, J. McDonough, J. Cha, C. S. Criddle and Y. Cui, *Energy Environ. Sci.*, 2011, **4**, 1293–1297.
144 M. Lu, S. Kharkwal, H. Y. Ng and S. F. Y. Li, *Biosens. Bioelectron.*, 2011, **26**, 4728–4732.
145 Y. Zhang, Y. Hu, S. Li, J. Sun and B. Hou, *J. Power Sources*, 2011, **196**, 9284–9289.
146 M. Lu, L. Guo, S. Kharkwal, H. N. Wu, H. Y. Ng and S. F. Y. Li, *J. Power Sources*, 2013, **221**, 381–386.
147 K. B. Liew, W. R. Wan Daud, M. Ghasemi, K. S. Loh, M. Ismail, S. S. Lim and J. X. Leong, *Int. J. Hydrogen Energy*, 2015, **40**, 11625–11632.
148 Y. Chen, Z. Lv, J. Xu, D. Peng, Y. Liu, J. Chen, X. Sun, C. Feng and C. Wei, *J. Power Sources*, 2012, **201**, 136–141.
149 J. Huang, N. Zhu, T. Yang, T. Zhang, P. Wu and Z. Dang, *Biosens. Bioelectron.*, 2015, **72**, 332–339.

150 T.-S. Song, D.-B. Wang, H. Wang, X. Li, Y. Liang and J. Xie, *Int. J. Hydrogen Energy*, 2015, **40**, 3868–3874.
151 S. Singh and N. Verma, *Int. J. Hydrogen Energy*, 2015, **40**, 5928–5938.
152 A. Modi, S. Singh and N. Verma, *Electrochim. Acta*, 2016, **190**, 620–627.
153 P. Wang, B. Lai, H. Li and Z. Du, *Bioresour. Technol.*, 2013, **134**, 30–35.
154 M. Ma, Y. Dai, J.-L. Zou, L. Wang, K. Pan and H.-G. Fu, *ACS Appl. Mater. Interfaces*, 2014, **6**, 13438–13447.
155 M. Ma, S. You, X. Gong, Y. Dai, J. Zou and H. Fu, *J. Power Sources*, 2015, **283**, 74–83.
156 R. Li, Y. Dai, B. Chen, J. Zou, B. Jiang and H. Fu, *J. Power Sources*, 2016, **307**, 1–10.
157 S. Khilari, S. Pandit, M. M. Ghangrekar, D. Das and D. Pradhan, *RSC Adv.*, 2013, **3**, 7902–7911.
158 X. Quan, Y. Mei, H. Xu, B. Sun and X. Zhang, *Electrochim. Acta*, 2015, **165**, 72–77.
159 Q. Wen, S. Wang, J. Yan, L. Cong, Z. Pan, Y. Ren and Z. Fan, *J. Power Sources*, 2012, **216**, 187–191.
160 G. Gnana kumar, Z. Awan, K. Suk Nahm and J. Stanley Xavier, *Biosens. Bioelectron.*, 2014, **53**, 528–534.
161 N. Garino, A. Sacco, M. Castellino, J. A. Muñoz-Tabares, A. Chiodoni, V. Agostino, V. Margaria, M. Gerosa, G. Massaglia and M. Quaglio, *ACS Appl. Mater. Interfaces*, 2016, **8**, 4633–4643.
162 Y. Hou, H. Yuan, Z. Wen, S. Cui, X. Guo, Z. He and J. Chen, *J. Power Sources*, 2016, **307**, 561–568.
163 X. Xie, G. Yu, N. Liu, Z. Bao, C. S. Criddle and Y. Cui, *Energy Environ. Sci.*, 2012, **5**, 6862–6866.
164 Z. He, J. Liu, Y. Qiao, C. M. Li and T. T. Y. Tan, *Nano Lett.*, 2012, **12**, 4738–4741.
165 C. Tang and Q. Zhang, *J. Mater. Chem. A*, 2016, **4**, 4998–5001.
166 R. Jasinski, *Nature*, 1964, **201**, 1212–1213.
167 F. Zhao, F. Harnisch, U. Schröder, F. Scholz, P. Bogdanoff and I. Herrmann, *Electrochem. Commun.*, 2005, **7**, 1405–1410.
168 E. H. Yu, S. Cheng, B. E. Logan and K. Scott, *J. Appl. Electrochem.*, 2008, **39**, 705–711.
169 Z. Chen, D. Higgins, A. Yu, L. Zhang and J. Zhang, *Energy Environ. Sci.*, 2011, **4**, 3167–3192.
170 F. Zhao, F. Harnisch, U. Schröder, F. Scholz, P. Bogdanoff and I. Herrmann, *Environ. Sci. Technol.*, 2006, **40**, 5193–5199.
171 L. Birry, P. Mehta, F. Jaouen, J. P. Dodelet, S. R. Guiot and B. Tartakovsky, *Electrochim. Acta*, 2011, **56**, 1505–1511.
172 H. Schulenburg, S. Stankov, V. Schünemann, J. Radnik, I. Dorbandt, S. Fiechter, P. Bogdanoff and H. Tributsch, *J. Phys. Chem. B*, 2003, **107**, 9034–9041.
173 R. Chen, H. Li, D. Chu and G. Wang, *J. Phys. Chem. C*, 2009, **113**, 20689–20697.
174 R. Burkitt, T. R. Whiffen and E. H. Yu, *Appl. Catal., B*, 2016, **181**, 279–288.
175 E. HaoYu, S. Cheng, K. Scott and B. Logan, *J. Power Sources*, 2007, **171**, 275–281.
176 Y. Yuan, B. Zhao, Y. Jeon, S. Zhong, S. Zhou and S. Kim, *Bioresour. Technol.*, 2011, **102**, 5849–5854.
177 Y. Yuan, J. Ahmed and S. Kim, *J. Power Sources*, 2011, **196**, 1103–1106.
178 Y. Zhang, G. Mo, X. Li and J. Ye, *J. Power Sources*, 2012, **197**, 93–96.
179 M.-T. Nguyen, B. Mecheri, A. Iannaci, A. D'Epifanio and S. Licoccia, *Electrochim. Acta*, 2016, **190**, 388–395.
180 S. Cheng, H. Liu and B. E. Logan, *Environ. Sci. Technol.*, 2006, **40**, 364–369.
181 J. R. Kim, J.-Y. Kim, S.-B. Han, K.-W. Park, G. D. Saratale and S.-E. Oh, *Bioresour. Technol.*, 2011, **102**, 342–347.
182 L. Deng, M. Zhou, C. Liu, L. Liu, C. Liu and S. Dong, *Talanta*, 2010, **81**, 444–448.
183 J. Ahmed, H. J. Kim and S. Kim, *RSC Adv.*, 2014, **4**, 44065–44072.
184 B. Li, X. Zhou, X. Wang, B. Liu and B. Li, *J. Power Sources*, 2014, **272**, 320–327.
185 B. Li, M. Wang, X. Zhou, X. Wang, B. Liu and B. Li, *Bioresour. Technol.*, 2015, **193**, 545–548.
186 M. H. Gerardi, *The microbiology of anaerobic digesters*, John Wiley & Sons, 2003.
187 H. Yuan, I. M. Abu-Reesh and Z. He, *J. Membr. Sci.*, 2016, **502**, 116–123.
188 J. Ahmed, Y. Yuan, L. Zhou and S. Kim, *J. Power Sources*, 2012, **208**, 170–175.
189 S. Gupta, D. Tryk, I. Bae, W. Aldred and E. Yeager, *J. Appl. Electrochem.*, 1989, **19**, 19–27.
190 Y. Zhao, K. Watanabe and K. Hashimoto, *J. Am. Chem. Soc.*, 2012, **134**, 19528–19531.
191 Y. Zhao, K. Watanabe and K. Hashimoto, *J. Mater. Chem. A*, 2013, **1**, 1450–1456.
192 X. Tang, H. Li, W. Wang, Z. Du and H. Y. Ng, *RSC Adv.*, 2014, **4**, 12789–12794.
193 Y. Su, H. Jiang, Y. Zhu, W. Zou, X. Yang, J. Chen and C. Li, *J. Power Sources*, 2014, **265**, 246–253.
194 X. Tang, H. Li, Z. Du and H. Y. Ng, *RSC Adv.*, 2015, **5**, 79348–79354.
195 S. Li, Y. Hu, Q. Xu, J. Sun, B. Hou and Y. Zhang, *J. Power Sources*, 2012, **213**, 265–269.
196 Y.-Z. Chan, Y. Dai, R. Li, J.-L. Zou, G.-H. Tian and H.-G. Fu, *Carbon*, 2015, **89**, 8–19.
197 Y. Pan, X. Mo, K. Li, L. Pu, D. Liu and T. Yang, *Bioresour. Technol.*, 2016, **206**, 285–289.
198 C. Santoro, A. Serov, C. W. Narvaez Villarrubia, S. Stariha, S. Babanova, A. J. Schuler, K. Artyushkova and P. Atanassov, *ChemSusChem*, 2015, **8**, 828–834.
199 H. Furukawa, K. E. Cordova, M. O'Keeffe and O. M. Yaghi, *Science*, 2013, **341**, 1230444.
200 G. Goenaga, S. Ma, S. Yuan and D.-J. Liu, *ECS Trans.*, 2010, **33**, 579–586.
201 S. Ma, G. A. Goenaga, A. V. Call and D.-J. Liu, *Chem. – Eur. J.*, 2011, **17**, 2063–2067.
202 E. Proietti, F. Jaouen, M. Lefèvre, N. Larouche, J. Tian, J. Herranz and J.-P. Dodelet, *Nat. Commun.*, 2011, **2**, 416.
203 A. Morozan and F. Jaouen, *Energy Environ. Sci.*, 2012, **5**, 9269–9290.

204 W. Xia, A. Mahmood, R. Zou and Q. Xu, *Energy Environ. Sci.*, 2015, **8**, 1837–1866.
205 H. Tang, S. Cai, S. Xie, Z. Wang, Y. Tong, M. Pan and X. Lu, *Adv. Sci.*, 2016, **3**, 1500265.
206 C. Santoro, A. Serov, C. W. N. Villarrubia, S. Stariha, S. Babanova, K. Artyushkova, A. J. Schuler and P. Atanassov, *Sci. Rep.*, 2015, **5**, DOI: 10.1038/srep16596.
207 P. Clauwaert, D. van der Ha, N. Boon, K. Verbeken, M. Verhaege, K. Rabaey and W. Verstraete, *Environ. Sci. Technol.*, 2007, **41**, 7564–7569.
208 K. Y. Cheng, G. Ho and R. Cord-Ruwisch, *Environ. Sci. Technol.*, 2010, **44**, 518–525.
209 S. Carbajosa, M. Malki, R. Caillard, M. F. Lopez, F. J. Palomares, J. A. Martín-Gago, N. Rodríguez, R. Amils, V. M. Fernández and A. L. De Lacey, *Biosens. Bioelectron.*, 2010, **26**, 877–880.
210 A. Cournet, M. Bergé, C. Roques, A. Bergel and M.-L. Délia, *Electrochim. Acta*, 2010, **55**, 4902–4908.
211 S. Parot, I. Vandecandelaere, A. Cournet, M.-L. Délia, P. Vandamme, M. Bergé, C. Roques and A. Bergel, *Bioresour. Technol.*, 2011, **102**, 304–311.
212 X.-W. Liu, X.-F. Sun, Y.-X. Huang, D.-B. Li, R. J. Zeng, L. Xiong, G.-P. Sheng, W.-W. Li, Y.-Y. Cheng, S.-G. Wang and H.-Q. Yu, *Biotechnol. Bioeng.*, 2013, **110**, 173–179.
213 S. Freguia, S. Tsujimura and K. Kano, *Electrochim. Acta*, 2010, **55**, 813–818.
214 M. Rosenbaum, F. Aulenta, M. Villano and L. T. Angenent, *Bioresour. Technol.*, 2011, **102**, 324–333.
215 K. Rabaey, S. T. Read, P. Clauwaert, S. Freguia, P. L. Bond, L. L. Blackall and J. Keller, *ISME J.*, 2008, **2**, 519–527.
216 B. E. Logan, *Nat. Rev. Microbiol.*, 2009, **7**, 375–381.
217 A. Venkataraman, M. A. Rosenbaum, S. D. Perkins, J. J. Werner and L. T. Angenent, *Energy Environ. Sci.*, 2011, **4**, 4550.
218 B. E. Morris, R. Henneberger, H. Huber and C. Moissl-Eichinger, *FEMS Microbiol. Rev.*, 2013, **37**, 384–406.
219 V. B. Wang, K. Sivakumar, L. Yang, Q. Zhang, S. Kjelleberg, S. C. J. Loo and B. Cao, *Sci. Rep.*, 2015, **5**, DOI: 10.1038/srep11222.
220 Z. He, J. Kan, F. Mansfeld, L. T. Angenent and K. H. Nealson, *Environ. Sci. Technol.*, 2009, **43**, 1648–1654.
221 L. Xiao, E. B. Young, J. A. Berges and Z. He, *Environ. Sci. Technol.*, 2012, **46**, 11459–11466.
222 S. J. You, N. Q. Ren, Q. L. Zhao, J. Y. Wang and F. L. Yang, *Fuel Cells*, 2009, **9**, 588–596.
223 J. Wei, P. Liang, X. Cao and X. Huang, *Bioresour. Technol.*, 2011, **102**, 10431–10435.
224 G.-D. Zhang, Q.-L. Zhao, Y. Jiao, J.-N. Zhang, J.-Q. Jiang, N. Ren and B. H. Kim, *J. Power Sources*, 2011, **196**, 6036–6041.
225 Y. Zhang, J. Sun, Y. Hu, S. Li and Q. Xu, *Int. J. Hydrogen Energy*, 2012, **37**, 16935–16942.
226 H. Tursun, R. Liu, J. Li, R. A. Abro, X. Wang, Y. Gao and Y. Li, *Front. Microbiol.*, 2016, **7**, 6.
227 C. Li, L. Ding, H. Cui, L. Zhang, K. Xu and H. Ren, *Bioresour. Technol.*, 2012, **116**, 459–465.
228 H. Zhang, R. Zhang, G. Zhang, F. Yang and F. Gao, *Int. J. Hydrogen Energy*, 2014, **39**, 11250–11257.
229 X.-W. Liu, X.-F. Sun, Y.-X. Huang, G.-P. Sheng, S.-G. Wang and H.-Q. Yu, *Energy Environ. Sci.*, 2011, **4**, 1422–1427.
230 L. Zhuang, Y. Yuan, G. Yang and S. Zhou, *Electrochem. Commun.*, 2012, **21**, 69–72.
231 Y. Zhang, J. Sun, Y. Hu, S. Li and Q. Xu, *J. Power Sources*, 2013, **239**, 169–174.
232 O. Schaetzle, F. Barriere and U. Schroder, *Energy Environ. Sci.*, 2009, **2**, 96–99.
233 H. Luo, S. Jin, P. H. Fallgren, H. J. Park and P. A. Johnson, *Chem. Eng. J.*, 2010, **165**, 524–528.
234 S. R. Higgins, C. Lau, P. Atanassov, S. D. Minteer and M. J. Cooney, *ACS Catal.*, 2011, **1**, 994–997.
235 C. Wu, X.-W. Liu, W.-W. Li, G.-P. Sheng, G.-L. Zang, Y.-Y. Cheng, N. Shen, Y.-P. Yang and H.-Q. Yu, *Appl. Energy*, 2012, **98**, 594–596.
236 A. Szczupak, D. Kol-Kalman and L. Alfonta, *Chem. Commun.*, 2012, **48**, 49–51.
237 C. Santoro, S. Babanova, P. Atanassov, B. Li, I. Ieropoulos and P. Cristiani, *J. Electrochem. Soc.*, 2013, **160**, H720–H726.
238 L. Zhang, X. Jiang, J. Shen, K. Xu, J. Li, X. Sun, W. Han and L. Wang, *RSC Adv.*, 2016, **6**, 29072–29079.
239 I. S. P. Savizi, H.-R. Kariminia and S. Bakhshian, *Environ. Sci. Technol.*, 2012, **46**, 6584–6593.
240 A. Ter Heijne, D. P. Strik, H. V. Hamelers and C. J. Buisman, *Environ. Sci. Technol.*, 2010, **44**, 7151–7156.
241 X. Xia, Y. Sun, P. Liang and X. Huang, *Bioresour. Technol.*, 2012, **120**, 26–33.
242 X. Xia, J. C. Tokash, F. Zhang, P. Liang, X. Huang and B. E. Logan, *Environ. Sci. Technol.*, 2013, **47**, 2085–2091.
243 H. Yuan and Z. He, *Bioresour. Technol.*, 2015, **195**, 202–209.
244 L. Malaeb, K. P. Katuri, B. E. Logan, H. Maab, S. P. Nunes and P. E. Saikaly, *Environ. Sci. Technol.*, 2013, **47**, 11821–11828.
245 Y. Li, L. Liu, F. Yang and N. Ren, *J. Membr. Sci.*, 2015, **484**, 27–34.
246 J. Liu, L. Liu, B. Gao, F. Yang, J. Crittenden and N. Ren, *Int. J. Hydrogen Energy*, 2014, **39**, 17865–17872.
247 Y. Li, L. Liu and F. Yang, *J. Membr. Sci.*, 2016, **505**, 130–137.
248 Y.-K. Wang, W.-W. Li, G.-P. Sheng, B.-J. Shi and H.-Q. Yu, *Water Res.*, 2013, **47**, 5794–5800.
249 T. Yu, L. Liu, Q. Yang, J. Song and F. Yang, *RSC Adv.*, 2015, **5**, 48946–48953.
250 J.-Y. Chen, N. Li and L. Zhao, *J. Power Sources*, 2014, **254**, 316–322.
251 S. C. Popat, D. Ki, B. E. Rittmann and C. I. Torres, *ChemSusChem*, 2012, **5**, 1071–1079.
252 X. Cao, X. Huang, P. Liang, K. Xiao, Y. Zhou, X. Zhang and B. E. Logan, *Environ. Sci. Technol.*, 2009, **43**, 7148–7152.
253 Y. Kim and B. E. Logan, *Desalination*, 2013, **308**, 122–130.
254 H. Liu, S. Grot and B. E. Logan, *Environ. Sci. Technol.*, 2005, **39**, 4317–4320.
255 Y. Zhang and I. Angelidaki, *Water Res.*, 2014, **56**, 11–25.
256 H. Yuan, J. Li, C. Yuan and Z. He, *ChemElectroChem*, 2014, **1**, 1828–1833.

257 Y. Hou, B. Zhang, Z. Wen, S. Cui, X. Guo, Z. He and J. Chen, *J. Mater. Chem. A*, 2014, **2**, 13795–13800.
258 X. Fan, Z. Peng, R. Ye, H. Zhou and X. Guo, *ACS Nano*, 2015, **9**, 7407–7418.
259 Y. Hou, S. Cui, Z. Wen, X. Guo, X. Feng and J. Chen, *Small*, 2015, **11**, 5940–5948.
260 Y. Hou, Z. Wen, S. Cui, S. Ci, S. Mao and J. Chen, *Adv. Funct. Mater.*, 2015, **25**, 872–882.
261 J. Lu, W. Zhou, L. Wang, J. Jia, Y. Ke, L. Yang, K. Zhou, X. Liu, Z. Tang, L. Li and S. Chen, *ACS Catal.*, 2016, **6**, 1045–1053.
262 Y. Hou, M. R. Lohe, J. Zhang, S. Liu, X. Zhuang and X. Feng, *Energy Environ. Sci.*, 2016, **9**, 478–483.